AD_____

Award Number: DAMD17-98-1-8564

TITLE: Prostate Specific Gene Therapy Using a 'Gutless' Adene-Vector Expressing Antisense TGF-Beta and PSA Promotor-Control

PRINCIPAL INVESTIGATOR: Arie Belldegrun, M.D.

CONTRACTING ORGANIZATION: University of California, Los Angeles
Los Angeles, California 90095-1406

REPORT DATE: September 1999

TYPE OF REPORT: Annual Summary

PREPARED FOR: U.S. Army Medical Research and Materiel Command
Fort Detrick, Maryland 21702-5012

REPORT DOCUMENTATION PAGE

Form Approved
OMB No. 074-0188

1. AGENCY USE ONLY (Leave blank)	2. REPORT DATE	3. REPORT TYPE AND DATES COVERED
	September 1999	Annual Summary (1 Sep 98 - 31 Aug 99)

4. TITLE AND SUBTITLE
Prostate Specific Gene Therapy Using a 'Gutless' Adene-Vector Expressing Antisense TGF-Beta and PSA Promotor-Control

5. FUNDING NUMBERS
DAMD17-98-1-8564

6. AUTHOR(S)
Arie Belldegrun, M.D.

7. PERFORMING ORGANIZATION NAME(S) AND ADDRESS(ES)
University of California, Los Angeles
Los Angeles, California 90095 -1406

e-mail:
abelldegrun@mednet.ucla.edu

8. PERFORMING ORGANIZATION REPORT NUMBER

9. SPONSORING / MONITORING AGENCY NAME(S) AND ADDRESS(ES)
U.S. Army Medical Research and Materiel Command
Fort Detrick, Maryland 21702-5012

10. SPONSORING / MONITORING AGENCY REPORT NUMBER

11. SUPPLEMENTARY NOTES
This report contains colored photos

12a. DISTRIBUTION / AVAILABILITY STATEMENT
Approved for public release
distribution unlimited

12b. DISTRIBUTION CODE

13. ABSTRACT ***(Maximum 200 Words)***

A gene therapy protocol that can achieve exquisite prostate cancer restricted expression of cytotoxic genes will minimize systemic side effects. Thus, we designed our prostate specific therapeutic scheme using the well-characterized Prostate Specific Antigen PSA enhancer/promoter (PSE). We have generated new constructs that increase the transcriptional activity greatly over the natural version. High in vivo expression coupled with its specificity will hold the best chance for effective therapy in patients. We have taken a combined approach of targeted cytotoxicity and generation of a tumor-specific immune response with reversal of local immunosuppression. We aim to achieve this gene therapy scheme with the most advanced 'gutless' adenovector (Δ-Ad) and likely the most effect vector for prostate cancer. We have made significant progress in the refinement of gutless Ad propagation. However, we will need continual improvement in this area. We will continue to improve on the blockade of transforming growth factor (TGF-β) expression with new antisense constructs. Evaluation of tumor necrosis factor (TNF-α) related cytokine with less systemic toxicity is actively pursued as likely candidate for prostate cancer therapy.

14. SUBJECT TERMS	15. NUMBER OF PAGES
Prostate	76
	16. PRICE CODE

17. SECURITY CLASSIFICATION OF REPORT	18. SECURITY CLASSIFICATION OF THIS PAGE	19. SECURITY CLASSIFICATION OF ABSTRACT	20. LIMITATION OF ABSTRACT
Unclassified	Unclassified	Unclassified	Unlimited

NSN 7540-01-280-5500

Standard Form 298 (Rev. 2-89)
Prescribed by ANSI Std. Z39-18
298-102

FOREWORD

Opinions, interpretations, conclusions and recommendations are those of the author and are not necessarily endorsed by the U.S. Army.

____ Where copyrighted material is quoted, permission has been obtained to use such material.

____ Where material from documents designated for limited distribution is quoted, permission has been obtained to use the material.

____ Citations of commercial organizations and trade names in this report do not constitute an official Department of Army endorsement or approval of the products or services of these organizations.

_✓__ In conducting research using animals, the investigator(s) adhered to the "Guide for the Care and Use of Laboratory Animals," prepared by the Committee on Care and use of Laboratory Animals of the Institute of Laboratory Resources, national Research Council (NIH Publication No. 86-23, Revised 1985).

_✓__ For the protection of human subjects, the investigator(s) adhered to policies of applicable Federal Law 45 CFR 46.

____ In conducting research utilizing recombinant DNA technology, the investigator(s) adhered to current guidelines promulgated by the National Institutes of Health.

____ In the conduct of research utilizing recombinant DNA, the investigator(s) adhered to the NIH Guidelines for Research Involving Recombinant DNA Molecules.

____ In the conduct of research involving hazardous organisms, the investigator(s) adhered to the CDC-NIH Guide for Biosafety in Microbiological and Biomedical Laboratories.

9.29.99

PI - Signature Date

Award Number: DAMD17-98-1-8564

TABLE OF CONTENTS

INTRODUCTION:

Our ultimate goal is to develop an immune-based gene therapy to successfully eradicate prostate cancer (CaP) cells *in situ.* We have taken a combined approach of targeted cytotoxicity and generation of a tumor-specific immune response with reversal of local immunosuppression. The most efficient vehicle to deliver gene products to the CaP tumor site is an adenoviral vector (Ad) (8-11). However, the development of cellular and humoral immune responses (14,15) against viral gene products utilizing first generation (E1-deleted) Ad would greatly hinder our immune-based gene therapy approaches. We therefore propose to develop a minimal immunogenic 'gutless' adenovector (Δ-Ad) for CaP which has all viral coding sequences deleted and which allows prostate-specific expression of a cytotoxic gene tumor necrosis factor (TNF-α) and an antisense transforming growth factor (TGF-β) RNA to reverse intratumoral immune suppression.

BODY:

Task 1. *To develop a "gutless adenoviral vector driven by PSA promoter/enhancer to improve safety and specificity of prostate cancer gene therapy.*

- *To develop the gutless viral system*

1. *Generation of "gutless" adenovirus constructs*

The structure of the "gutless" adenovector is shown schematically in figure 1. The *gutless* adenovector was

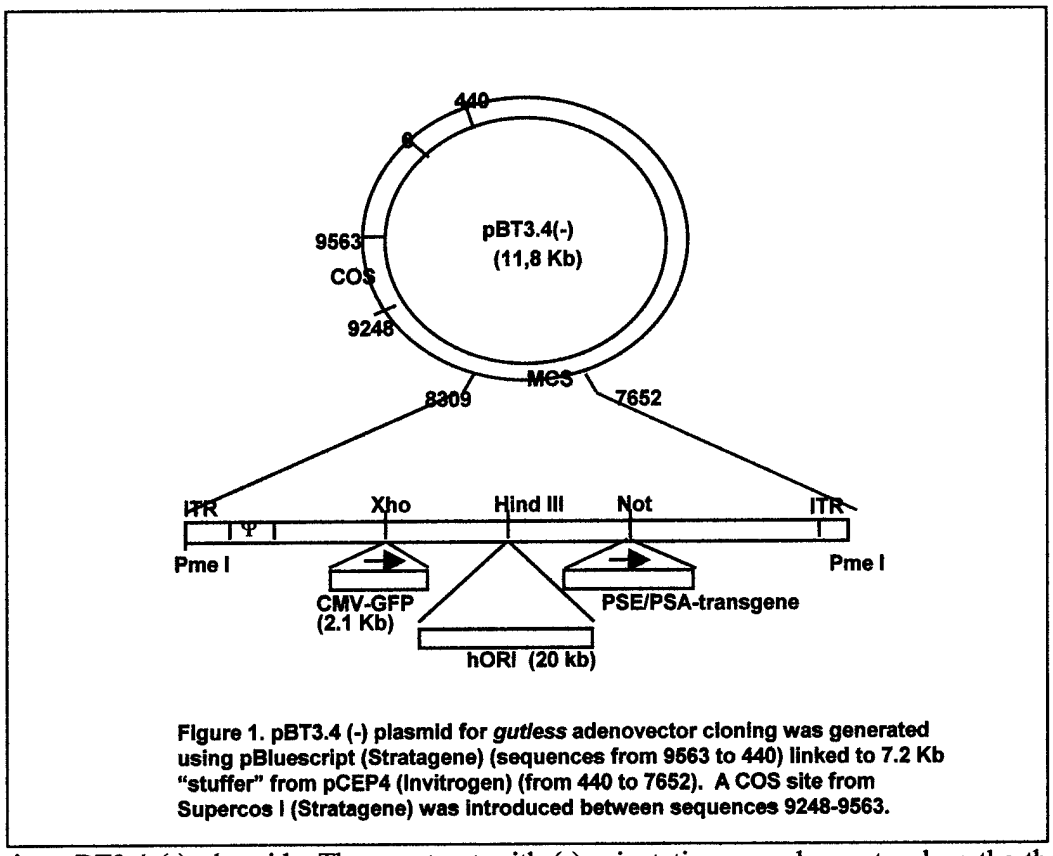

Figure 1. pBT3.4 (-) plasmid for *gutless* adenovector cloning was generated using pBluescript (Stratagene) (sequences from 9563 to 440) linked to 7.2 Kb "stuffer" from pCEP4 (Invitrogen) (from 440 to 7652). A COS site from Supercos I (Stratagene) was introduced between sequences 9248-9563.

generated using pBT3.4 (-) plasmid. The construct with (-) orientation was chosen to place the therapeutic transgene(s) far from the adenoviral left terminus in order to minimize influences of adenoviral E1 enhancer sequences. To facilitate the titration and evaluation of transduction efficiency of our *gutless* adenoviral vector, we introduced marker green fluorescence protein (GFP) gene driven by CMV promoter into Xho I site of pBT3.4 (-). pBT3.4 plasmid was engineered with a cos site inserted between sequences 9248 and 9563 to facilitate the cloning and selection of large plasmid containing 20 Kb "stuffer" plus therapeutic gene(s). The "stuffer" fragment, originated from pLIB41-Not I plasmid, is the 20 Kb human ORI gene cloned into Hind III site. This step of cloning was carried out in the cosmid packaging system (Gigapack III Gold from Stratagene) and the total size of *gutless* adenoviral vector was approximately 34 Kb. The therapeutic

transgenes will be cloned in the Not I site and the final *gutless* adenovector construct will be released by digestion with PmeI prior to transfection with helper virus.

2. *Modification of helper virus*

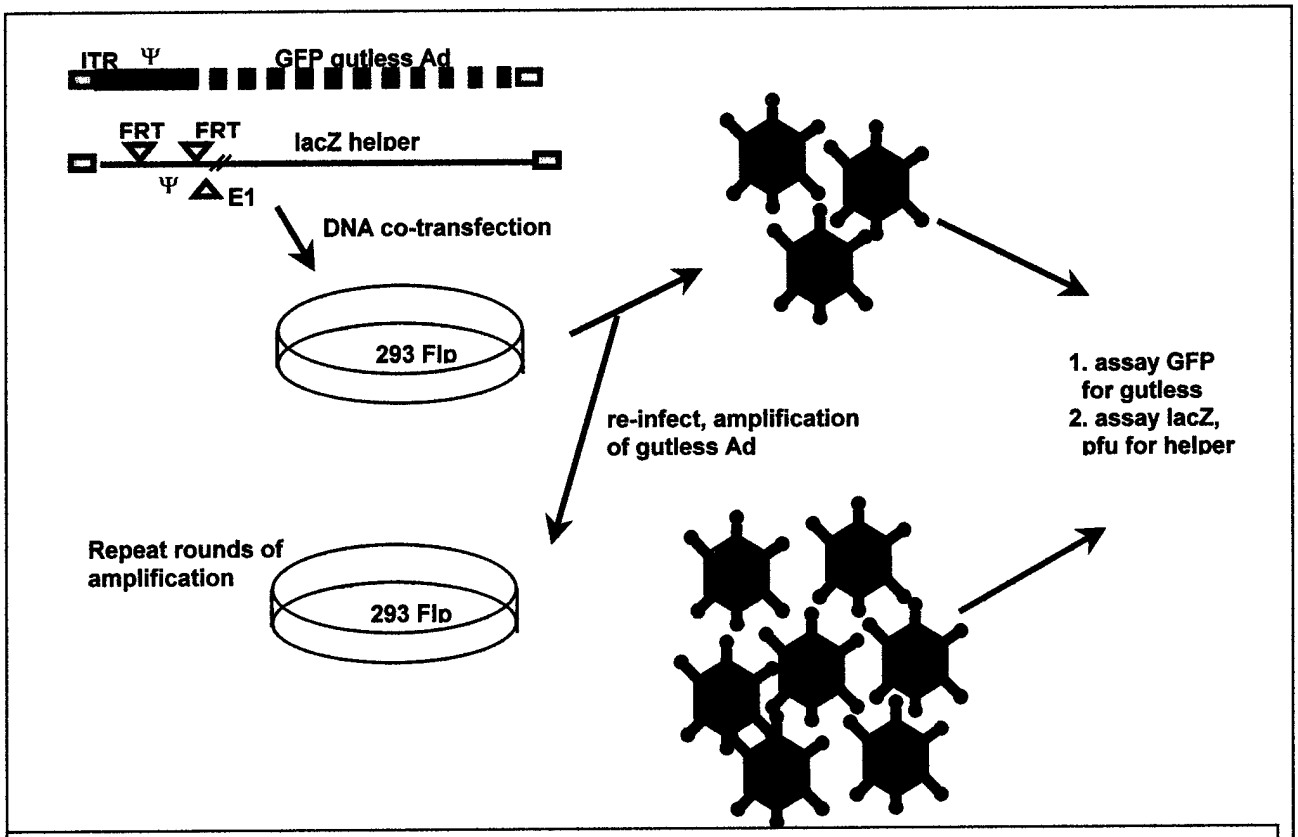

Figure 2. Growth and amplification of gutless Ad. Gutless Ad vector DNA are co-transfected with helper virus DNA into 293Flp cells. Cell lysates are harvested after 3 days and used to infect 293Flp cells in subsequent rounds of amplification. The gutless Ad titers can be assayed by linked marker gene, GFP. Helper virus contamination can be analyzed by plaque formation or linked marker gene, β-galatosidase.

The scheme of 'gutless' Ad propagation is shown in figure 2. The helper virus contains the β-galactosidase marker gene which will allow convenient and facile tracking of helper virus contamination during amplification of the gutless Ad (figure 2). This helper virus we generated (figure 3A) also processes two FRT sites flanking the packaging signal which renders it un-packageable in 293FLP.

3. Characterization of 293Flp cell line

We have further characterized the 293Flp cell, clone 51 and its subclone 51T, to evaluate the efficiency of Flp mediated recombination, i.e. excision of packaging signal from helper virus. We attempted to alter various cell-culturing conditions to improve Flp recombination efficiency. We demonstrated that excision is more efficient at 32°C than at 37°C, 88% vs 80% respectively (figure 3B). This result is logical since Flp, a yeast derived protein,

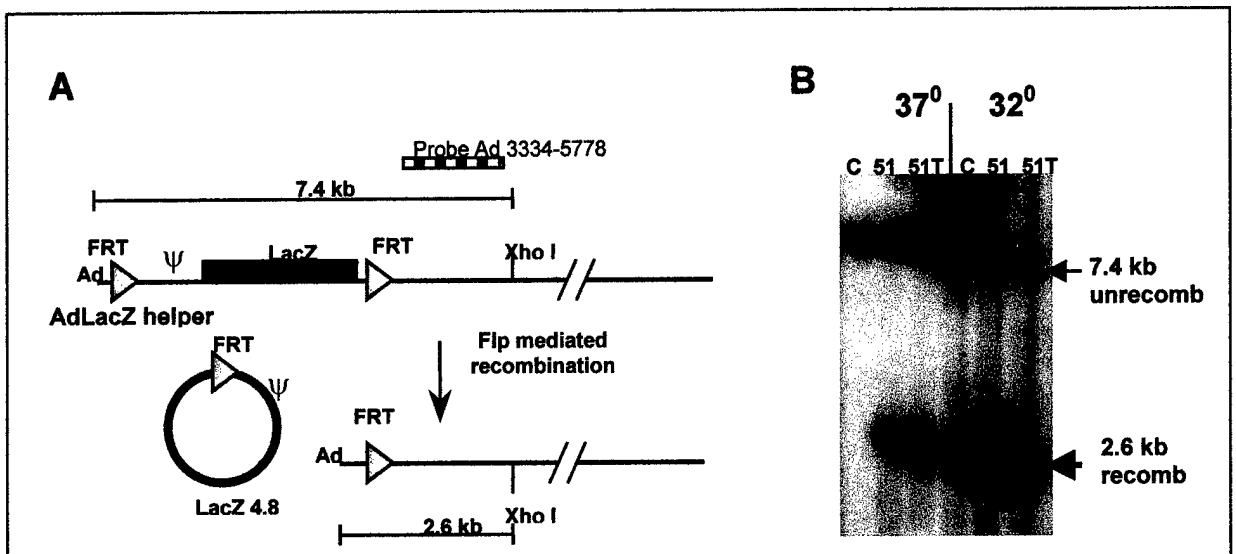

Figure 3. Recombination of AdLacZ helper virus in 293Flp Cells. A. structure of helper virus and expected recombination
products detected on Southern blot after XhoI restriction digest of viral DNA with adenoviral sequence 3334-5778 as probe. B. Optimization of Flp recombination at varying temperature. Quantitation of the blot indicates recombination is 88% vs 80% complete at 32^0 vs 37^0 respectively. 293Flp cell clone 51T is a subclone of clone 51

probably function optimally at the lower growth temperature of yeast. We also tried to reversibly block viral DNA replication as this approach could keep the input helper viral template low for Flp to complete its function before viral replication proceeds resulting in greatly amplified viral templates. However, our attempt with use of hydoxyurea to reversibly inhibit replication also resulted in complete blockage of Flp recombination (data not shown).

4. Gutless virus propagation

We proceeded to use the helper virus and 293Flp cells (described above) to propagate a gutless adenovirus containing the GFP marker gene (ΔAd-GFP). The backbone of this gutless Ad is derived from Dr. Kochanek's

vector, pSTK120 with large genomic sequence from human HGPRT locus (). The ΔAd-GFP titer, assayed by green flourescence transducing units (gtu), expanded quite well after the initial co-transfection and subsequent rounds of amplification by co-infection (figure 4). However, the helper virus titer assayed by lacZ expression and plaque formation also continued to expand with no diminution after second round (figure 4). This result indicates that the functional level of Flp in 293Flp cell is probably insufficient to greatly incapacitate the packaging of the helper virus. To overcome this problem, we plan to generate 293Flp cells where the level of Flp expression can be amplified greatly with linkage to inducible locus such as dhfr ( ).

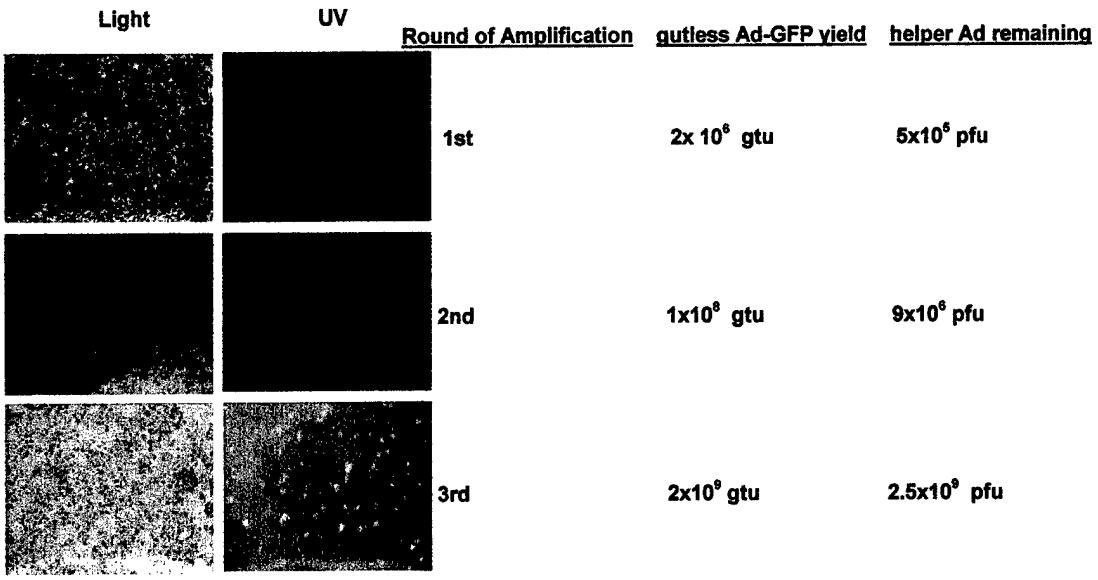

Figure 4. Growth and Amplification of gutless Ad-GFP with 293Flp system. First round of growth was initiated after co-transfection of 293Flp cells and subsequent rounds were performed with co-infection of gutless Ad-GFP and helper virus. Gutless virus yield after each round was assayed by gene transfer units (gtu). As shown in left panels, cell lysates from each round were used to infect 293 cells and enumerate the green flourescent cells under microscopy with UV illumination. Helper virus content was established by plaque forming units (pfu) or β-galactosidase histochemical staining.

- *Evaluation of tissue specific expression of the adenoviral construct*

We have worked diligently to optimize the expression of PSA enhancer/promoter driven transgene, as high efficiency and specificity of transduction would most likely result in effective in vivo gene therapy. Our preliminary results indicate the natural PSA enhancer/promoter activity in adenovector is quite low compared to cytomegalovirus promoter (CMV), about 20 fold lower (figure 5). Herpes simplex virus thymidine kinase gene (TK) was utilized in adenovectors (AdCMV-TK and AdPSE-TK) such that we could follow in vivo gene transfer in living animals by PET imaging ( ).

We have constructed several new PSA enhancer/promoter constructs to increase the promoter activity. Due to the ongoing patent application of these new constructs, their detail structures will not be disclosed at this time. Two of the new constructs express the linked marker gene, luciferase, nearly 20 times higher than the native

PSA enhancer/promoter (PSE, -5322 to –2875 and –541 to +11) in LNCaP cells in the presence of synthetic androgen R1881 (figure 6). The most potent construct is greatly enhanced in androgen induction, 1745 fold, compared to PSE, 428 fold (figure 7). Importantly, the new constructs retain strict prostate specificity as expression in non prostate cells, Hela (cervical carcinoma) or MCF-7 (breast carcinoma) is negligible.

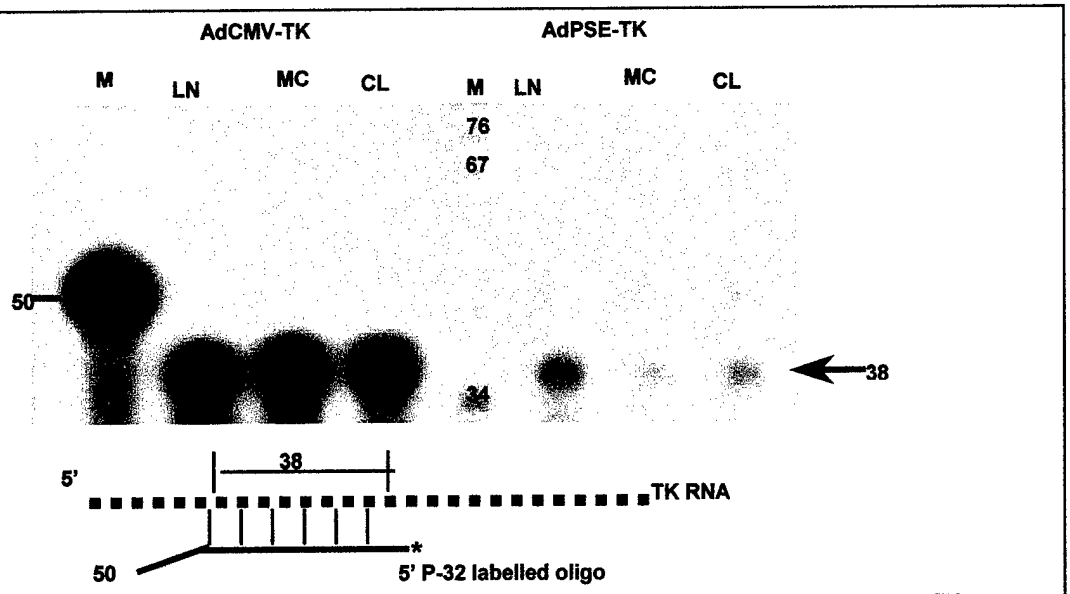

Figure 5. S1 protection analysis of TK RNA. Cells were infected with AdCMV-TK or AdPSE-TK at MOI of 5. 48 hrs. post infection, cytoplasmic RNA were harvested and subjected to S1 analysis. Unprotected TK 5' end labelled oligonucleotide probe is 50 bases. TK mRNA transcribed from the CMV or PSE promoter would expect to protect a 38 bases probe fragment. TK RNA expressed from the CMV promoter are similar to all cells and are 20-30x higher than TK RNA expressed from PSE in LNCaP and CL-2 cells. TK RNA from PSE in LNCaP is 3-5x higher than in MCF-7.
M=marker, LN=LNCaP, MC=MCF-7 and CL=CL-2 cells.

Task 2. *Evaluation of anti-tumor effects of anti-sense TGF-β constructs in vitro*

We have demonstrated that TGF-β is over-expressed in high-grade prostate tumors and correlates closely with the occurrence of metastasis and poor prognosis. The immunoregulatory properties of TGF-β include inhibition of T-cell mediated tumor cytotoxicity *in vitro* and *in vivo*, inhibition of IL-2-dependent T-cell proliferation, and impairment of lymphokine-activated killer and natural killer cell activation. TGF-β antagonizes the immune stimulatory effects of IL-2 by down-regulation of IL-2 receptors. TGF-β also mediates angiogenesis by up-regulating vascular endothelial growth factor (VEGF) and basic fibroblast growth factor (bFGF). Although the exact mechanisms of action of TGF-β in tumor cells are still under investigation, its role as an immune suppressive factor has been demonstrated in malignant gliomas, head and neck, ovarian and prostate cancers.

Immune surveillance is one of the major defense mechanisms against cancer. Thus increasing the immunogenicity of tumor by down regulating the potent immune suppressor TGF-β can lead to a local anti-tumor effect and enhance the efficacy of combined immune-based gene therapy. To achieve this goal, we used TGF-β

antisense to bind and inactivate TGF-β mRNA translation in prostate tumor cells. A major advantage of this strategy over conventional drug treatment is its specificity to correct cellular and genetic alterations in tumor

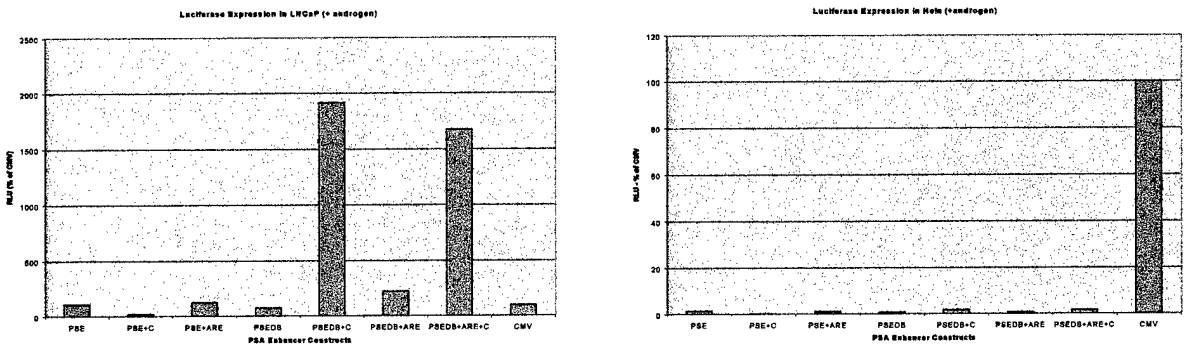

Figure 6. Activity of new PSA enhancer constructs. Transcriptional activity of all constructs were measured by luciferase activity after transfection by lipofectamine. I nM R1881 was added to culture media supplemented with charcoal stripped serum. Promoter activities are represented relative to CMV (=100%). PSE is the native PSA enhancer (-5322 to -2875) and promoter (-541 to +11).

cells. The TGF-β antisense plasmid vectors pCEP4/TGF-β were constructed with 18-21 bp DNA fragments corresponding to different regions of human TGF–β1 and TGF-β2 cDNA and inserted in reverse orientation into BamH I and Hind III sites of the plasmid vector pCEP4 (Invitrogen, CA). In using short antisense RNAs, we are attempting to increase the specificity of our antisenses in avoiding extensive secondary structures formed by target mRNA. Six short antisenses (figure 8A) were designed in an attempt to identify one that would specifically reduce TGF-β expression and modify cellular properties. Three antisenses complementary to the region of the start codon, including the ribosome-binding site, were constructed (AS-1, AS-2, AS-3) as this is usually a more accessible site for protein-binding and initiation of translation. Three other antisenses were directed to the region of homology of TGF–β1 and TGF–β2. Corresponding control vectors were constructed in sense orientation. The expression of TGF-β antisense sequence in pCEP4 is driven by CMV promoter and the vector also contains the hygromycin resistance gene. Two prostate cancer cell lines (PC-3; CL1) and bladder cancer cells (T24) were transfected with pCEP4/TGF-β antisense vectors. Pools of clones were selected from cultures with increasing amounts of hygromycin up to 200 μg/ml (Sigma, MO).

The efficacy of antisense constructs in inhibiting TGF–β1 and TGF–β2 expression was first evaluated in total cell RNA isolated from tumor cells by RT-PCR. The selectivity of TGF-β antisenses for their targeted proteins was further measured in culture supernatants by enzyme-linked immunosorbent assay (ELISA, R&D Systems) in duplicate and compared to control groups.

Short TGF-β antisense RNAs inhibit between 40% (AS-5) to 22% (AS-1, AS-2, AS-4) of TGF-β2 in T24 cells but did not inhibit significantly TGF-β2 expression in two prostate tumor cell lines tested (Fig.8B, C). Possibly

the 18-21 bp antisense sequences transcribed from pCEP4 plasmid might be too short to recognize TGF-β mRNA or the long polyA tail that follows the antisenses might obscure the accessibility to their targets. Although our initial goal was to increase the specificity and facilitate the binding of short antisenses in open target sequences of TGF-β2 mRNA secondary structure, they appeared to be ineffective.

We will take two alternative approaches to overcome this problem. We will construct two TGF-β antisenses using the same vector but containing a 300 bp DNA (PCR-amplified) fragment corresponding to the start codon region of TGF-β2 cDNA (ATCC, VA) and a 150 bp DNA fragment corresponding to the region of homology

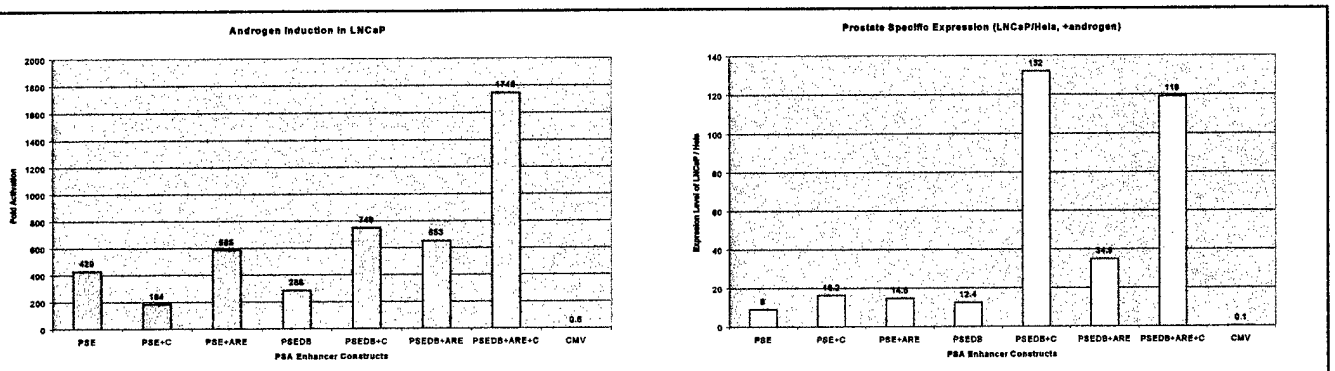

Figure 7. Prostate specificity of new PSA enhancer constructs. Transcriptional activity of all constructs were measured in LNCaP (prostate cells) or Hela (cervical carcinoma) after transfection in culture media with 10% charcoal stripped serum (no androgen) or with 1 nM R1881. Androgen induction represents luciferase activity in the presence of androgen over no androgen. Prostate specificity was Calculated using luciferase activity in LNCaP over Hela.

between TGF–β1 and TGF-β2. We will also test short, synthetic strands of DNA antisenses with modified phosphate backbones to retard nuclease degradations. Phosphorothioates have one oxygen replaced by a sulfur atom in the phosphate backbone. Phosphorothioate oligonucleotides have been studied extensively *in vitro*, *in vivo* and in clinical trials for several cancer models. Its lack of toxicity and relative stability *in vivo* has made antisense phosphorothioates oligonucleotides an excellent specific therapeutic agent.

Task 3. *Evaluation of anti-tumor effects of Ad-TNF-α both in vivo and in vitro*

TNF-α significantly upregulated the expression of HLA class I and intracellular adhesion molecule (ICAM) I antigens in CaP cells (Belldegrun, Cancer). Additionally, TNF-α treatment led to reduction in c-myc, epidermal growth factor receptor, PSA, and AR expression levels. Other pleiotropic anti-tumor effects of TNF-α included direct cytotoxicity, induction of hemorrhagic necrosis in addition to immune-modulation. Although clearly the most potent cytokine with anti-tumor activity *in vitro* and *in vivo,* discovered so far, the clinical utility of TNF-α has been limited by its tremendous systemic toxicity and due to insufficient delivery of TNF-α to the tumor site. We proposed to restrict TNF-α expression to CaP tissue using our prostate-specific PSE in an Ad vector. Alternatively, we have also explored the use of TNF-related protein (TNF related apoptosis inducing ligand, TRAIL) which

appeared to induce apoptosis more specifically in tumor cells and not in normal cells (10). The tumoricidal activity of TRAIL was recently demonstrated in vivo in a mammary carcinoma model in SCID mice (38). The result that no significant systemic toxicity was observed in the animals is quite encouraging.

TRAIL or Apo-2 ligand is a member of the TNF superfamily (14) whose amino acid sequence showed high

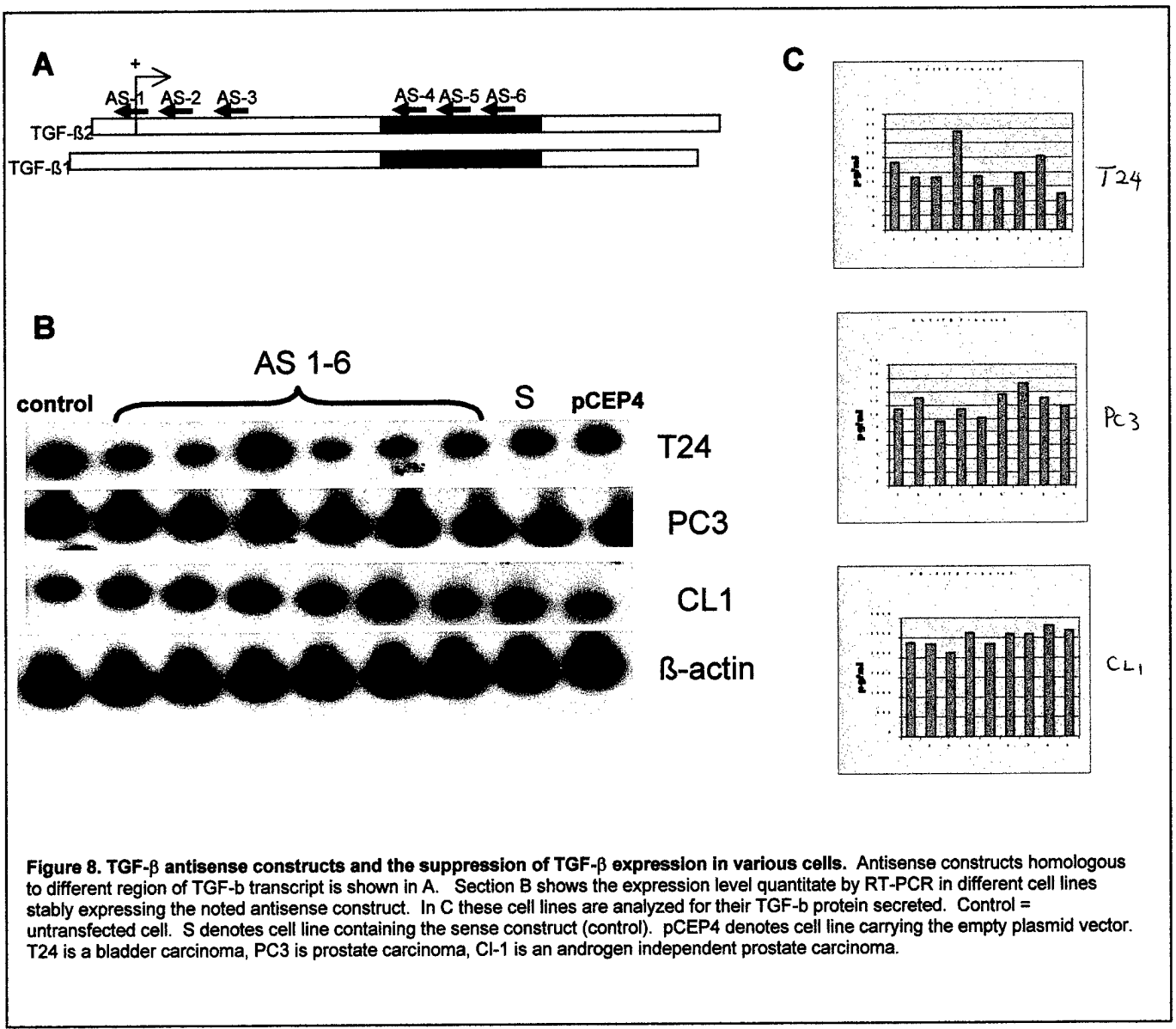

Figure 8. TGF-β antisense constructs and the suppression of TGF-β expression in various cells. Antisense constructs homologous to different region of TGF-b transcript is shown in A. Section B shows the expression level quantitate by RT-PCR in different cell lines stably expressing the noted antisense construct. In C these cell lines are analyzed for their TGF-b protein secreted. Control = untransfected cell. S denotes cell line containing the sense construct (control). pCEP4 denotes cell line carrying the empty plasmid vector. T24 is a bladder carcinoma, PC3 is prostate carcinoma, Cl-1 is an androgen independent prostate carcinoma.

homology to TNF-α and Fas-ligand. The mechanism of TRAIL mediated tumor selective apoptosis with sparing of normal cells is unclear. The multiple TRAIL receptors and decoy receptors and their complex downstream signalling cascade certainly contribute to the intricate control of this apoptotic pathway. A molecule with potent tumoricidal effect yet non-toxic to normal tissue will be of extreme important to the field of cancer therapeutics. We review the utility of TRAIL as a potential therapeutic agent in a paper titled "Tumor Necrosis factor-related

apotosis-inducing ligand (TRAIL) for treatment of Prostate Cancer: first results and review of the literature" (in press in Prostate Can & Prostat Dis, 1999, manuscript enclosed in appendices section).

We have also developed an androgen independent prostate cancer cell line such that we can use our gene therapy scheme to treat this aggressive disease in animals. This cell line is characterized in detail and submitted for publication in an article titled 'Androgen Deprivation Induces Outgrowth of Aggressive Hormone Refractory Prostate Cancer Clones Expressing Distinct Cellular and Molecular Properties Not Present in Parental Androgen-Dependent Cancer Cells' (manuscript enclosed in appendices section).

KEY RESEARCH ACCOMPLISHMENTS:

- **Gutless adenovectors are under construction**
- **Helper virus has been generated**
- **Cell line to propagate gutless Ad has been generated and further characterized**
- **New PSA enhancer promoter constructs have been generated with greatly increased activity yet retain exquisite tissue specificity**
- **Evaluation of TGF-b antisense constructs has been ongoing**
- **Careful analysis of a TNF-a related cytokine with potential much less systeimic toxicity for use in prostate cancer therapy**
- **Generation of an aggressive androgen independent prostate cancer cell line and tumor model**

REPORTABLE OUTCOMES:

1. Manuscript: "Tumor Necrosis factor-related apotosis-inducing ligand (TRAIL) for treatment of Prostate Cancer: first results and review of the literature" (in press in Prostate Can & Prostat Dis, 1999)
2. Manuscript: "Androgen Deprivation Induces Outgrowth of Aggressive Hormone Refractory Prostate Cancer Clones Expressing Distinct Cellular and Molecular Properties Not Present in Parental Androgen-Dependent Cancer Cells" submitted
3. Patent application in progress on the CL-1 and CL-2 cell line and tumor model
4. Patent application in progress on the new PSA enhancer/promoter constructs

CONCLUSIONS:

A gene therapy protocol that can achieve exquisite prostate cancer restricted expression of cytotoxic genes will minimize systemic side effects. Thus, we designed our prostate specific therapeutic scheme using the well-characterized Prostate Specific Antigen PSA enhancer/promoter (PSE). We have generated new constructs that increase the transcriptional activity greatly over the natural version. High in vivo expression coupled with its specificity will hold the best chance for effective therapy in patients. We have taken a combined approach of targeted cytotoxicity and generation of a tumor-specific immune response with reversal of local immunosuppression. We aim to achieve this gene therapy scheme with the most advanced 'gutless' adenovector (Δ-Ad) and likely the most effect vector for prostate cancer. We have made significant progress in the refinement of gutless Ad propagation. However, we will need continual improvement in this area. We will continue to improve on the blockade of transforming growth factor (TGF-β) expression with new antisense constructs. Evaluation of tumor necrosis factor (TNF-α) related cytokine with less systemic toxicity is actively pursued as likely candidate for prostate cancer therapy.

BIBLIOGRAPHY

1. van Ophoven A, Ng C, Patel B, Bonavida B, **Belldegrun A**: Tumor Necrosis factor-related apoptosis-inducing ligand (TRAIL) for treatment of prostate cancer: first results and review of the literature. Prostate Cancer and Prostatic Diseases (submitted 7/99).

2. Tso C-L, McBride W, Sun J, Patel B, Tsui K-H, Paik S, Gitlitz B, Caliliw R, van Ophoven A, Wu L, deKernion J, **Belldegrun A**: Androgen Deprivation Induces Selective Outgrowth of Aggressive Hormone Refractory Prostate Cancer Clones Expressing Distinct Cellular and Molecular Properties not Present in Parental Androgen-Dependent Cancer Cells. Cancer Research (submitted 8/99)

Award Number: DAMD17-98-1-8564

PERSONNEL LIST

Lily Wu, MD, PhD, Assistant Professor of Urology

Cho-Lea Tso, MA, Research Specialist

Frederick Dorey, PhD, Biostatistician

Amnon Zisman, MD, Postdoctoral Fellow

Tumor Necrosis factor-related apoptosis-inducing ligand (TRAIL) for treatment of Prostate Cancer: first results and review of the literature

Arndt van Ophoven, Chuen Pei Ng, Belur Patel,
Benjamin Bonavida and Arie Belldegrun

Summary

Purpose: We present the involvement and association of TNF-related apoptosis-inducing ligand (TRAIL) with apoptosis. Its potential applications as a therapeutic agents in urologic oncology is discussed.

Materials and Methods: We have examined the sensitivity of prostate carcinoma cell lines DU145, PC3 and LNCaP to TRAIL-induced apoptosis and the expression of TRAIL receptors. Furthermore we looked into the sensitization of those prostate carcinoma cell lines to TRAIL-mediated apoptosis by low toxic levels of Actinomycin-D. Furthermore, we review and discuss the pertinent literature on the molecular biology of TRAIL, its receptors and future potential for therapy in urologic oncology.

Results: Recent discovery and characterization of TRAIL has led to further broadening and insights into the apoptotic process. Based on preceding *in vitro* studies the first *in vivo* study using TRAIL has been conducted and published in 1999. Systemic application of TRAIL in SCID mice resulted in tumor regression of subcutaneous implanted mammary and colon cancer and several groups are looking into TRAIL sensitivity of prostate cancer and renal cancer cellines. Our *in vitro* data revealed a significant increase of apoptotic cell death rate following the combined application of TRAIL with Actinomycin-D.

Conclusions: Our results suggest that the combination of TRAIL and ActD may be a therapeutic option in the treatment of drug/hormone refractory prostate carcinoma. In the future TRAIL may be used in combination therapy with other immunotherapies or gene therapies providing a synergistic effect or enhancing the efficacy of chemotherapeutic or radiotherapeutic regimens.

Introduction

Programmed cell death called apoptosis helps in the elimination of unwanted cells, in contrast to necrosis which is not a physiological process. Apoptosis occurs during embryonal development and plays an important role in immunoregulation, tumor biology and tissue physiology. Cell death as a physiological pathway has been described and studied over 150 years, initially with the study of metamorphosis in amphibians (1). The initial studies were based on the idea that the observed cell death occurred basically secondarily to tissue damage. The idea that cell death is a genetically controlled process in normal cells did not come until the late 1980's. Studies with the nematode *Caenorhabditis elegans* proved the theory that cell death was a genetically controlled pathway in normal cells, leading to new insights into the idea of programmed cell death (2, 3). Distinct morphological features are noted in apoptotic cells like membrane blebbing, cellular shrinkage and condensation of chromatin which can be easily detected under the microscope. The biochemically processes leading to cell death by the apoptotic pathway is via the translocation of phosphatidylserine in the outer layer of cell membrane and the activation of endonuclease which cleaves genomic DNA into multiple internucleosomal fragments. In contrast, cell necrosis is based on noxious stimulants such as temperature, radiation, oxidation or trauma and not on genetically controlled pathways. On the cellular level necrosis is characterized by mitochondrial damage and cell lysis.

Defects in programmed cell death play a major role in the pathogenesis of tumors allowing neoplastic cells to survive beyond their normally intended lifespans. Deficiencies in apoptosis also contribute to carcinogenesis by creating a permissive environment for genetic instability and accumulation of gene mutations. These mutations in turn permit dysregulation of cell cycle checkpoints which would normally induce apoptosis. Also these changes will facilitate growth factor and hormone independent cell survival, supporting anchorage independent survival during metastasis(4). Therefore, strategies to interfere with the process of anti-apoptosis or to overcome its effects will be beneficial in cancer therapy.

Recent discoveries of a new apoptosis-inducing molecule and its receptors has led to further broadening and insights into the apoptotic process. This molecule is part of the Tumor Necrosis Factor (TNF) superfamily and is called TNF-related apoptosis-inducing ligand (TRAIL) or APO2-L. This review discusses the biochemical characteristics and molecular biology of TRAIL and its receptors and their implication in cancer treatment.

TNF and TRAIL

TNF is a cytokine which plays an important role in acute and chronic inflammation and is also a mediator in endotoxic shock. It is mainly produced by T cells, natural killer cells (NK cells) and activated macrophages. It was first discovered in the blood of BCG infected mice after they had been injected with endotoxin (5). TNF has been shown to be cytotoxic for tumor cells *in vitro* and to cause hemorrhagic necrosis of tumors in mice (6-10). Since 1985 TNF has been available to medical oncology, but its systemic application in patients with advanced tumor diseases failed because of toxicities. The high systemic toxicities resulted in low maximal tolerated doses, rare tumor remissions and organ failure 11, 12). Due to these problems clinical applications of TNF were limited though interest in its potential continued.

Between 1995 and 1996 two independent groups identified and characterized a new membrane protein (10, 13), whose amino acid sequence showed a 23% similarity to TNF-α and a 28% similarity to Fas-ligand (also known as Apo-1-ligand), which is a member of the TNF superfamily (14). Thus, this new protein was grouped in the TNF superfamily and was called TRAIL or Apo-2-ligand, because of its similarity to Fas-ligand. TRAIL is a 281 amino acid protein with its C terminus exposed, indicating a type II transmembrane protein topology. The extracellular domaine of TRAIL is homologous to that of other family members. The discovery and subsequent cloning of TRAIL was based on bioinformatic analysis of expressed sequence tag (EST) databases which contain amino acid sequences of proteins that are expressed by the human genome, and whose function are undetermined. The characterization and subsequent cloning of TRAIL was based on the comparison of conserved TNF sequences with a particular EST database (10, 13).

TRAIL and Apoptosis

Based on the comparison of the crystalline structure of TNF it was initially suggested that TRAIL had its highest biological activity as a trimer (15). Wiley et. al. proved this by showing that the soluble form of TRAIL, when multimeric or crosslinked, led to a higher induction of apoptosis when compared to the monomeric molecule (10). These studies also revealed a very unique characteristic and quality of TRAIL in that it appeared to induce apoptosis only in tumorigenic or transformed cells but not in normal cells *in vitro*. Moreover, TRAIL is expressed by a wide range of tissues like lymphocytes, spleen, prostate, ovary, colon and placenta, whereas TNF expression is more restricted and only transient in activated cells (10). Because of the discovery of different tissues expressing TRAIL it was suggested that the regulation of TRAIL-induced apoptosis was controlled by a restrictive expression of a single TRAIL receptor.

TRAIL and its receptors

The first TRAIL receptor was identified and cloned again with the help of an EST database in 1997 and was called TRAIL-R1 (16). This protein showed several identical characteristics to the receptors of the TNF-superfamily and was thus also called death receptor 4 (DR4) (in continuation of previously discovered TNF-DR1-3). TRAIL-R1 is a type I membrane protein with two extracellular cysteine rich pseudorepeats. Its cytoplasmatic part is made up of a death domain (DD) which signals and induces apoptosis (Figure 1). Again, the DD of TRAIL-R1 also shows a high similarity to the known death domain of the TNF receptors. Shortly after the discovery of TRAIL-R1, a second receptor, TRAIL-R2 or DR5 was identified (17-19). Its amino acid sequence shows a 58% similarity to TRAIL-R1 and is a type I transmembrane proteine with two extracellular cysteine pseudorepeats and a cytoplasmic DD. Since most tissues express both TRAIL-R1 and -R2 it has become apparent that the ligand and receptor system of TRAIL is far more complex than first anticipated leaving the reason for the tumor selectivity of TRAIL unclear at that time.

The complexity of the TRAIL system grew with the discovery of two further receptors, but this knowledge also led to the information about cell sensitivity and resistance to TRAIL (17, 18, 20-22). The two receptors TRAIL-R3 and R4 showed a 58% and 54%, 58% and 57% similarity to TRAIL-R1 and -R2, respectively, as well as a 70% similarity between themselves. However, the importance of the R3 and R4 lies not in the similarities to R1 and R2, but in their differences. In contrast to R1 and R2, R3 contains neither an intracellular DD nor a transmembranous domain, and is glycosylphophatidylinositol (GPI) -anchored to the cell surface. R4 differs in that it only has a truncated DD and does not signal for apoptosis. However, the four receptors are capable of binding TRAIL with comparable binding affinity. Thus TRAIL-R3 and R4 can compete with TRAIL-R1 and R2 for the TRAIL molecule without inducing apoptosis. The genes of the four TRAIL receptors are tightly clustered on human chromosome 8p21-22 suggesting that they evolved recently via gene duplication (20-22). The expression of TRAIL-R4 in various tissues is almost comparable to TRAIL-R1 and R2, while that of TRAIL-R3 is more limited (17, 18, 20).

TRAIL Sensitivity and Resistance

The discovery of expression of TRAIL and its receptors in normal cells led to doubts in the theory that regulation of TRAIL induced apoptosis was controlled by restrictive expression of receptors. The possibility of regulation by different receptor affinity was also excluded because all the receptors showed comparable binding affinities. (20, 21).

The first hypothesis on TRAIL sensitivity and resistance was based on the receptors R3 and R4 being devoid of functioning DD and that these receptors act as decoy receptors (DcR) by binding to TRAIL but not inducing apoptosis. This theory was supported by the fact that a) the DcRs were almost exclusively found in normal healthy cells and b) by transfection studies using TRAIL sensitive tumor cell lines. After transfection with either TRAIL-R3/DcR1 or TRAIL R4/DcR2 a decrease of apoptotic cell death was observed with a greater effect seen in DcR2 transfection (21). Although this theory was intriguing the discovery of TRAIL sensitive tumor cell lines expressing DcRs

and TRAIL resistant tumor cell lines without DcRs implied a more extensive and complicated pathway. Moreover, recent screening experiments of more than 60 human tumor cell lines showed no definitive correlation between the mRNA expression of the different TRAIL receptors and TRAIL sensitivity (23). Though mRNA expression does not necessarily imply cell surface expression, studies with monoclonal antibodies specific for TRAIL receptors supported the PCR data (23).

An alternative hypothesis for the explanation of different TRAIL sensitivity of tumor cells and normal cells was based on TRAIL-R4's ability to induce intracellular *anti*-apoptotic signals. Activation of nuclear factor kappa B (NF-κB) protects cells from TNF induced cell death probably due to upregulation of one or more genes resulting in cell resistance to apoptosis (24, 25). Binding of TRAIL-R4 leads to NF-κB activation and thus a possible reason for TRAIL resistance (21). On the other hand TRAIL-R1 and R2 have been shown to activate NF-κB without any antiapoptotic effect (26, 27), thus suggesting that the TRAIL sensitivity and resistance is not solely based on TRAIL-R4 and NF-κB.

The most complex theory is based on the interaction of different activators and inhibitors of cell death machinery. Initial studies of TRAIL-induced apoptotic pathways focused on the possible similarities to TNF and Fas death receptor pathways. These pathways involve the binding of Fas-associated-DD (FADD) proteins either directly (FADD mediated) or indirectly (TNF-R1-associated-DD (TRADD) mediated) leading to activation of apoptotic cell death (Figure 2). Binding to either of these adaptor molecules leads to activation of the caspase-cascade resulting in apoptopic cell death (28-30). Caspases, which constitute the key effector molecules for apoptotic pathways, are synthesized as inactive cysteine proteasen comprising an N-terminal peptide together with one large and one small subunit. Activation of caspases by proteolytic cleavage results in the cleavage of critical cellular substrates, precipitating the morphological changes of apoptosis (31).

The exact mechanism TRAIL-mediated cell death in association with FADD/TRADD continues to remain unclear because of contradictory data involving the binding of the adaptor molecules to TRAIL-R1 and R2. *In vitro* studies have shown both, no binding of

FADD/TRADD to TRAIL receptor (16-18), as well as binding (26, 27). The discrepancy between the two study results may be due to different expression levels of the adaptor molecules in the transfectans used in the experiments. Even though early data appears conflicting, the theory of activation of caspase cascade via FADD or TRADD by TRAIL still provides the most promising explanation for TRAIL-induced apoptosis. Further support for this theory has been shown indirectly by in vitro studies blocking caspase inhibitors and resulting in an increased TRAIL sensitivity (32). However the possibility of more extracellular and intracellular factors involved in cell apoptosis still exists (33).

TRAIL and p53

Tumor suppression is known to be partly in control of the p53 gene which regulates cell cycle and apoptosis. In the event of chromosomal damage p53 inhibits further cell replication and induces cell death. The exact mechanism of cell death induction is still unclear (34, 35).

The TRAIL and TNF superfamily apoptotic pathways were initially thought to be independent of p53. However, recent studies have shown an association of p53 to the Fas-ligand (36) and more recently its relationship to the TRAIL receptor (37, 38). The studies cloned a p53-dependent gene which was induced by DNA damage called KILLER gene. This KILLER gene was identical to the TRAIL-R2 gene. The KILLER/TRAIL-R2 gene was highly expressed in DNA damaged cells when overexpression of a wild-type p53 transgene occurred. Tumor cells with p53 mutations did not show expression of the KILLER gene. This led to the conclusion that p53 is involved in the TRAIL receptor and caspase apoptotic cell death pathway. The involvement of p53 gene leads to further questions such as the influence of p53 on TRAIL-R2 expression and the role of p53/TRAIL-interaction in apoptotic regulation.

Therapeutic Potentials of TRAIL

Based on the *in vitro* studies, Walczak et. al. have conducted the first *in vivo* study using TRAIL. The study looked at the toxicity and efficacy of TRAIL in SCID mice injected with mammary cancer MDA-231. After intravenous injection of 500μg human

TRAIL and 1mg murine TRAIL no significant toxicity was seen with mice viability, tissue integrity and blood count (39).

When TRAIL was given to mice with either subcutaneous or intraperitoneal (ip) tumors a significant longer survival was noted in mice with ip administered TRAIL as compared to control (69days vs. 35.5 days). The effect of tumor regression was noted to be dose-dependent and when the mice with subcutaneous MDA-231 tumors were given 500μg of TRAIL daily for ten days, iv or ip, the tumor was undetectable in 80% and 100% of the mice, respectively, after 40 days. Similar results were obtained with two human colon carcinomas, COLO-205 and HCT-15 (39). The authors showed that the effect of TRAIL was based on immediate apoptosis in all three malignancies.

We have recently reported studies performed *in vitro* on the sensitivity of AIDS-Kaposi's sarcoma to TRAIL-mediated apoptosis. AIDS-KS are resistant to killing by chemotherapeutic drugs and cytotoxic effector lymphocytes. The acquisition of anti-apoptotic characteristics by AIDS-KS cells may contribute to their prolonged survival. We examined the sensitivity of ten different isolates of AIDS-KS to TRAIL-mediated apoptosis and found they were all relatively resistant. However, combination of TRAIL and Actinomycin-D (ActD) resulted in a synergistic cytotoxic activity in nine of the ten samples. We also demonstrated the involvement of BCL-XL selectively in the sensitization of AIDS-KS to TRAIL-induced apoptosis (40). These findings suggest that the combination of TRAIL and ActD may be a potential option in the treatment of AIDS-KS.

TRAIL and Prostate Cancer

We have also recently examined the sensitivity of prostate carcinoma cell lines to TRAIL-induced apoptosis and the expression of TRAIL receptors by RT-PCR. Table 1 summarizes the expression of TRAIL receptors on PC3, DU145 and LNCaP cells. All three cell lines express the four receptors at different levels. Furthermore, all three cell lines were resistant to TRAIL-mediated apoptosis. However, when the cells were treated with ActD they became sensitized to apoptosis (Figure 3). These results suggest that the

combination of TRAIL and ActD may be a therapeutic option in the treatment of drug/hormone refractory prostate carcinoma. (Ng et al., in preparation).

Conclusions

The impressive *in vivo* and *in vitro* results open new therapeutic options for cancer. The therapeutic option of directly inducing the cell death pathway via the TRAIL receptors has many implications and provides a promising future in antitumor therapy. A p53-independent induction of apoptosis is a promising therapeutic approach, because of the high amount of human tumors with p53 mutations. Moreover, targeting of death receptors for tumor therapy is attractive, because of their p53-independent induction of the caspase-cascade. Recent *in vitro* studies showed a caspase-associated apoptosis-induction in several in prostate and renal cell carcinoma (41-44). Several chemotherapeutics aim at DNA damage resulting in subsequent p53-induction. Others, particularly anthracyclines, have been demonstrated to activate caspases through a variety of mechanisms (45, 46). The combination of those chemotherapeutics with TRAIL may increase the anti-proliferative effect of the single drug via synergy or activation of additional apoptotic signaling. Recent *in vitro* data showed a significant increase of apoptotic cell death rate following the combined application of TRAIL with doxorubicin, 5-fluoruracil (47), adriamycin, taxol or etoposide (48). The augmentation of caspase activation observed may be due to its amplification upon reception of two independent activating signals. However, the exact mechanism is yet not known. TRAIL may be also used in combination therapy with other immunotherapies or gene therapies providing a synergistic effect or enhancing the efficacy of another therapeutic regimen. Moreover, it can be used as monotherapy for treatment of tumors either systemically or by direct intratumoral application in the absence of toxicity. The discovery of TRAIL as part of the TNF superfamily and its impressive results again opens the door for the study of the role of TNF and its superfamily in cells and will provide further knowledge of cell and tumor biology.

Literature

1. Vogt C: Untersuchungen über die Entwicklungsgeschichte der Geburtshelferkröte (*Alytes obstetricans*). 1842. Zitiert in Jacobson, MD; Weil, M; Raff, MC. Programmed cell death in animal development. Cell 1997, 88:347-54
2. Horvitz, HR; Shaham, S; Hengartner, MO. The genetics of programmed cell death in the nematode Caenorhabditis elegans. Cold Spring Harb Symp Quant Biol 1994, 59:377-85
3. Ellis, HM; Horvitz, HR. Genetic control of programmed cell death in the nematode C. elegans. Cell 1986, 44 (6):817-29
4. Reed, JC. Mechanisms of apoptosis avoidance in cancer. Cur Opin Oncol 1999, 11(1):68-75
5. Carswell, EA; Old, LJ; Kassel, RL; Green, S; Fiore, N; Williamson, B. An endotoxin-induced serum factor that causes necrosis of tumors. Proc Natl Acad Sci USA 1975, 72 (9):3666-70
6. Old, LJ. Tumor necrosis factor (TNF). Science 1985, 230:630-2
7. Vassalli, P. The pathophysiology of tumor necrosis factors. Annu Rev Immunol 1992, 10:411-52
8. Tracey, KJ; Cerami, A. Tumor necrosis factor, other cytokines and disease. Annu Rev Cell Biol 1993, 9:317-43
9. Bazzoni, F; Beutler, B. The tumor necrosis factor ligand and receptor families. New Engl J Med 1996, 334:1717-25
10. Wiley, SR; Schooley, K; Smolak, PJ; Din, WS; Huang, CP; Nicholl, JK; Sutherland, GR; Smith, TD; Rauch, C; Smith, CA: Goodwin; RG. Identification and characterization of a new member of the TNF family that induces apoptosis. Immunity 1995, 3(6):673-82
11. Creaven, PJ; Brenner, DE; Cowens, JW; Huben, RP; Wolf, RM; Takita, H; Arbuck, SG; Razack, MS; Proefrock, AD. A phase I clinical trial of recombinant human tumor necrosis factor given daily for five days. Cancer Chemther Pharmacol, 1989, 23(3):186-91

12. Wiedenmann, B; Reichardt, P; Räth, U; Theilmann, L; Schüle, B; Ho, AD; Schlick, E; Kempeni, J; Hunstein, W; Kommerell, B. Phase-I trial of intravenous continuous infusion of tumor necrosis factor in advanced metastatic carcinomas. J Cancer Res Clin Oncol, 1989, 115(2):189-92

13. Pitti, RM; Marsters, SA; Ruppert, S; Donahue, CJ; Moore, A; Ashkenazi, A. Induction of apoptosis by Apo-2 ligand, a new member of the tumor necrosis factor cytokine family. J Biol Chem 1996, 271(22):12687-90

14. Suda, T; Takahashi, T; Golstein, P; Nagata, S. Molecular cloning and expression of the Fas ligand, a novel member of the tumor necrosis factor family. Cell 1993, 75 (6):1169-78

15. Banner, DW; D'Arcy, A; Janes, W; Gentz, R; Schoenfeld, HJ; Broger, C; Loetscher, H; Lesslauer, W. Crystal structure of the soluble human 55 kd TNF receptor-human TNF beta complex: implications for TNF receptor activation. Cell 1993, 73(3):431-45.

16. Pan, G; O'Rourke, K; Chinnaiyan, AM; Gentz, R; Ebner, R; Ni, J; Dixit, VM. The receptor for the cytotoxic ligand TRAIL. Science 1997, 276:111-3

17. Pan, G; Ni, J; Wei, YF; Yu, G; Gentz, R; Dixit, VM. An antagonist decoy receptor and a death domain-containing receptor for TRAIL. Science 1997, 277:815-8

18. Sheridan, JP; Marsters, SA; Pitti, RM; Gurney, A; Skubatch, M; Baldwin, D; Ramakrishnan, L; Gray, CL; Baker, K; Wood, WI; Goddard, AD; Godowski, P; Ashkenazi, A. Control of TRAIL-induced apoptosis by a family of signaling and decoy receptors. Science 1997, 277:818-21

19. Walczak, H; Degli-Esposti, MA; Johnson, RS; Smolak, PJ; Waugh, JY; Boiani, N; Timour, MS; Gerhart, MJ; Schooley, KA; Smith, CA; Goodwin, RG; Rauch, CT. TRAIL-R2: a novel apoptosis-mediating receptor for TRAIL. Embo 1997, 16(17):5386-97

20. Degli-Esposti, MA; Smolak, PJ; Walczak, H; Waugh, J; Huang, CP; DuBose, RF; Goodwin, RG; Smith, CA. Cloning and characterization of TRAIL-R3, a novel ember of the emerging TRAIL receptor family. J Exp Med 1997, 186(7):1165-70

21. Degli-Esposti, MA; Dougall, WC; Smolak, PJ; Waugh, JY; Smith, CA; Goodwin, RG. The novel receptor TRAIL-R4 induces NF-kappaB and protects against TRAIL-mediated apoptosis, yet retains an incomplete death domain. Immunity 1997, 7(6):813-20

22. Marsters, SA; Sheridan, JP; Pitti, RM; Huang, A; Skubatch, M; Baldwin, D; Yuan, J; Gurney, A; Goddard, AD; Godowski, P; Ashkenazi, A. A novel receptor for Apo2L/TRAIL contains a truncated death domain. Cur Bio 1997, 7(12):1003-6

23. Griffith, TS; Lynch, DH. TRAIL: a molecule with multiple receptors and control mechanisms. Cur Opin Immun 1998, 10(5):559-63

24. Beg, AA; Baltimore, D. An essential role for NF-kappaB in preventing TNF-alpha-induced cell death. Science 1996, 274:782-4

25. Van Antwerp, DJ; Martin, SJ; Kafri, T; Green, DR; Verma, IM. Suppression of TNF-alpha-induced apoptosis by NF-kappaB. Science 1996 274:787-9

26. Chaudhary, PM; Eby, M; Jasmin, A; Bookwalter, A; Murray, J; Hood, L. Death receptor 5, a new member of the TNFR family, and DR4 induce FADD-dependent apoptosis and activate the NF-kappaB pathway. Immunity 1997, 7(6):821-30

27. Schneider, P; Thome, M; Burns, K; Bodmer, JL; Hofmann, K; Kataoka, T; Holler, N; Tschopp, J. TRAIL receptors 1 DR4 and 2 DR5 signal FADD-dependent apoptosis and activate NF-kappaB. Immunity 1997, 7(6):831-6

28. Wallach, D; Boldin, M; Goncharov, T; Goltsev, Y; Mett, I; Malinin, N; Adar, R; Kovalenko, A; Varfolomeev, E. Exploring cell death mechanisms by analyzing signaling cascades of the TNF/NGF receptor family. Behring Inst Mitt 1996, 97:144-55

29. Chinnaiyan, AM; Dixit, VM. The cell-death machine. Curr Biol, 1996, 6(5):555-62

30. Nagata, S. Apoptosis by death factor. Cell 1997, 88:355-65

31. Cohen, GM. Caspases: the executioners of apoptosis. Biochem J 1997, 326:1-16

32. Irmler, M; Thome, M; Hahne, M; Schneider, P; Hofmann, K; Steiner, V; Bodmer, JL; Schreoter, M; Burns, K; Mattmann, C; Rimoldi, D; French, LE; Tschopp, J. Inhibition of death receptor signals by cellular FLIP. Nature 1997, 388:190-5

33. Emery, JG; McDonnell, P; Burke, MB; Deen, KC; Lyn, S; Silverman, C; Dul, E; Appelbaum, ER; Eichman, C; DiPrinzio, R; Dodds, RA; James, IE; Rosenberg, M; Lee, JC; Young, PR. Osteoprotegerin is a receptor for the cytotoxic ligand TRAIL. J Bio Chem 1998, 273:14363-7

34. Levine, AJ. p53, the cellular gatekeeper for growth and division. Cell 1997, 88(3):323-31

35. Bates, S; Vousden, KH. p53 in signaling checkpoint arrest or apoptosis. Curr Opin Genet Dev 1996, 6(1):12-8

36. Müller, M; Strand, S; Hug, H; Heinemann, EM; Walczak, H; Hofmann, WJ; Stremmel, W; Krammer, PH; Galle, PR. Drug-induced apoptosis in hepatoma cells is mediated by the CD95 APO-1/Fas receptor/ligand system and involves activation of wild-type p53. J Clin Invest 1997, 99(3):403-13

37. Wu, GS; Burns, TF; McDonald, ER 3rd; Jiang, W; Meng, R; Krantz, ID; Kao, G; Gan, DD; Zhou, JY; Muschel, R; Hamilton, SR; Spinner, NB; Markowitz, S; Wu, G; el-Deiry, WS. KILLER/DR5 is a DNA damage-inducible p53-regulated death receptor gene. Nature Gen 1997, 17(2):141-3

38. Sheikh, MS; Burns, TF; Huang, Y; Wu, GS; Amundson, S; Brooks, KS; Fornace, AJ Jr; el-Deiry, WS. p53-dependent and -independent regulation of the death receptor KILLER/DR5 gene expression in response to genotoxic stress and tumor necrosis factor alpha. Cancer Res 1998, 58(8):1593-8.

39. Walczak, H; Miller, RE; Ariail, K; Glinika, B; Griffith, TS; Kubin M; Chin, W; Jones, J; Woodward, A; Le, T; Smith, C; Smolak, P; Goodwin, RG; Rauch, CT; Schuh, J; Lynch, DH. Tumoricidal activity of tumor necrosis factor-related apoptosis-inducing ligand in vivo. Nature Med 1999, 5(2):157-63

40. Mori, S.; Murakami-Mori, K.; Nakamura, S.; Ashkenazi, A.; and Bonavida, B. Sensitization of AIDS-Kaposi's sarcoma cells to APO-2 ligand-induced apoptosis by actinomycin-D. J Immunology, 1999, 162: 5616-5623

41. Horie, S; Kano, M; Higashihara, E; Moriyama, N; Tanaka, E; Hirose, A; Kakizoe, T; Kawabe, K. Expression of Fas in renal cell carcinoma. Jap J Clin Onc 1997, 27(6):384-8

42. Hedlund, TE; Duke, RC; Schleicher, MS; Miller, GJ. Fas-mediated apoptosis in seven human prostate cancer cell lines. Prostate 1998, 36(2):92-101

43. Marcelli, M; Cunningham, GR; Walkup, M; He, Z; Sturgis, L;Kagan, C; Mannucci, R; Nicoletti, I; Teng, B; Denner, L. Signalling pathway activated during apoptosis of the prostate cancer cell line LnCaP: Overexpression of caspase-7 as a new gene therapy strategy for prostate cancer. Cancer Res 1999, 59:382-390

44. Mandlekar, S; Yu, S; Ruben, S; Ni, J; Kong A-NT. TRAIL induces apoptosis in TNF-α-resistant PC-3 prostate cancer cells. Proc Am Ass Cancer Res 1999, 40: 168

45. Ferrari, D; Stepczynska, A; Los, M; Wesselborg, S; Schulze-Osthoff, K. Differential regulation and ATP requirement for caspase-8 and caspase-3 activation during CD95- and anticancer drug-induced apoptosis. J Exp Med 1998, 188(5):979-84

46. Hannun, YA. Apoptosis and the dilemma of cancer chemotherapy. Blood 1997, 89(6):1845-53

47. Keane, MM; Ettenberg, SA; Nau, MM; Russel, EK; Lipkowitz S. Chemotherapy augments TRAIL-induced apoptosis in breast cell lines. Cancer Res 1999, 59: 734-41

48. Kim, KH; el-Deiry WS. Molecular determinants of response to TRAIL combined with chemotherapy in killing of normal and cancer cells. Proc Am Ass Cancer Res 1999, 40: 486

49. Ashkenazi, A; Dixit, VA. Death receptors: Signaling and Modulation. Science 1998, 281:1305-8

50. Schulze-Osthoff, K; Ferrari, D; Los, M; Wesselborg S; Peter, ME. Apoptosis signaling by death receptors. Eur J Biochem. 1998 254:439-59

Figure 1

Schematic representation of the four TRAIL receptors. The two extracellular boxes represent the cysteine rich pseudorepeats (50).

Figure 2

Putative cell death pathway from TRAIL receptors1 and 2 (23, 49, 50).

DED = Death effector domain

DD = Death domain

FLIP = FLICE inducing ligand

CrmA = Cytokine response modifier A

zVDA = carbobenzyloxy [z] VAD

Figure 3

Sensitization of prostate carcinoma cell lines DU145, PC3 and LNCaP to TRAIL-mediated apoptosis by low toxic levels of Actinomycin-D (ActD). The cells were treated in 0, 10, 50, 100ng/ml ActD in combination with or without TRAIL (50ng/ml) for 24 hours. The cells were subsequently stained with propidium iodide (50mg/ml) and sub-G1 (apoptotic) fraction was determined by one-color cell cycle flow cytometric analysis. (◆, untreated; ●, treated with 50ng/ml TRAIL)

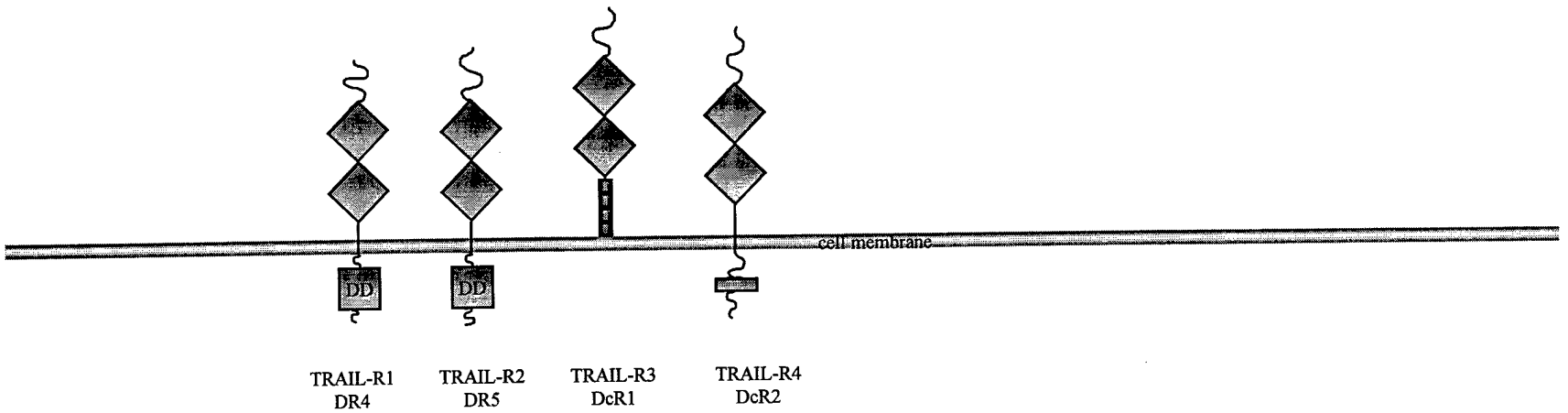
cell membrane
DD
DD
TRAIL-R1
DR4
TRAIL-R2
DR5
TRAIL-R3
DcR1
TRAIL-R4
DcR2

Fig 1.

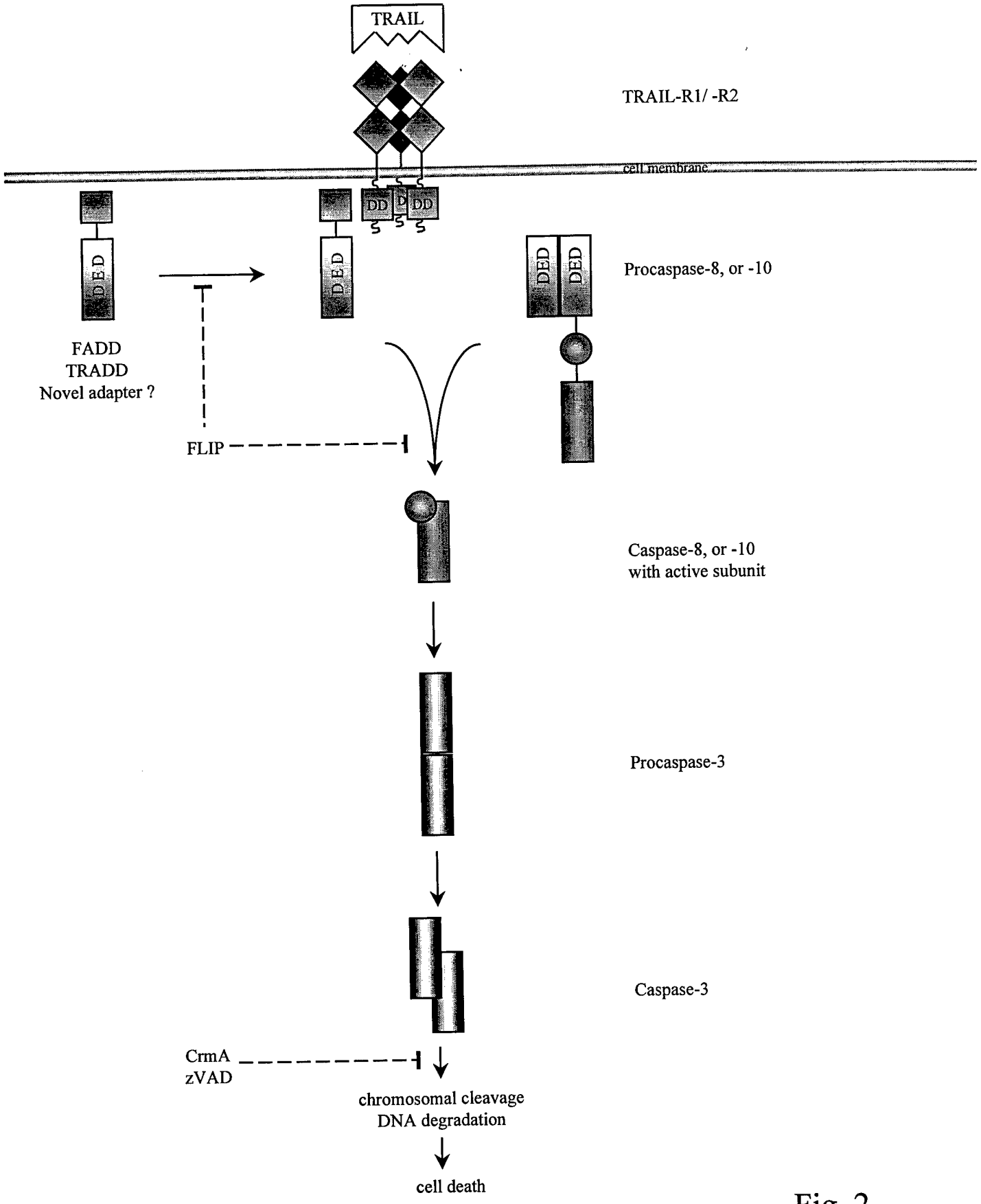
TRAIL
TRAIL-R1/ -R2
cell membrane
DD
D
DD
DED
DED
DED
DED
Procaspase-8, or -10
FADD
TRADD
Novel adapter ?
FLIP
Caspase-8, or -10
with active subunit
Procaspase-3
Caspase-3
CrmA
zVAD
chromosomal cleavage
DNA degradation
cell death

Fig. 2

Table 1. TRAIL receptor expression in prostate carcinoma cell lines.

Cell line	Expression of TRAIL receptor mRNA*				Sensitivity to TRAIL killing
	DR4	DR5	DcR1	DcR2	
PC3	+++	+	+	+	Resistant
DU145	++++	-	++	++++	Resistant
LNCaP	++	+	+	+++	Resistant

*Receptor expression was determined by RT-PCR. The level of the receptor mRNA expression was compared to the mRNA level of GAPDH. (-, 0-5% of GAPDH; +, 5-25% of GAPDH; ++, 25%-50% of GAPDH; +++, 50-75% of GAPDH; ++++, 75-100% of GAPDH). **Resistant indicates < 5.0 % killing at 500 ng/ml TRAIL.

Androgen Deprivation Induces Selective Outgrowth of Aggressive Hormone Refractory Prostate Cancer Clones Expressing Distinct Cellular and Molecular Properties Not Present in Parental Androgen- Dependent Cancer Cells

Cho-Lea Tso[1,3], William H. McBride[2,3], Jirong Sun[2,3], Belur Patel[1,3], Ke-Hung Tsui[1,3], Sun H. Paik[1,3], Barbara Gitlitz[1,3], Randy Caliliw[1,3], Arndt van Ophoven[1,3], Lily Wu[1,3], Jean deKernion[1,3], and Arie Belldegrun[1,3]

[1]Department of Urology, [2]Department of Radiation Oncology and [3]Jonsson Comprehensive Cancer Center, University of California Los Angeles, Los Angeles, California 90095

Running title: Selective growth of prostate cancer clones with aggressive phenotype by hormone deprivation treatment

Key words: prostate cancer, hormonal therapy, hormonal refectory, autocrine growth factors, angiogenic factors

Correspondence should be addressed to:

Arie Belldegrun, MD, FACS
Professor of Urology
UCLA School of Medicine
Department of Urology
CHS 66-118
Los Angeles, CA 90095-1738

Tel (310) 206-1434
Fax (310) 206-5343
abelldeg@ucla.edu

The abbreviations used are: CaP, prostate cancer; AI, androgen independent; AD, androgen dependent; AR, androgen receptors; PSA, prostate specific antigen; PSAM, prostate specific membrane antigen; GFP, green fluorescent protein; RT-PCR, quantitative reverse transcriptase-polymerase chain reaction; b-FGF, basic fibroblast growth factor; IL, interleukin; VEGF, vascular endothelial cell growth factor; TGF-β, transforming growth factors-beta; EGF-R, epidermal growth factor receptor; HRPC, hormonal refractory prostate cancer; RPMI, Roswell Park Memorial Institute; FACS, fluorescence-activated cell sorter; dNTP, deoxyribonucleosid triphosphate; AMV, avian myeloblastosis virus.

Abstract

The mechanism of progression of human prostate cancer (CaP) cells under androgen ablation therapy remains unclear. To study the alternative pathways of CaP cell growth under conditions of androgen-deprivation, a highly aggressive androgen-independent (AI) tumor line with distinct cellular and molecular properties, designated CL1, was selected and expanded from the androgen-dependent (AD) LNCaP cell line. Re-culturing CL1 cells in an androgen containing medium, designated CL2, resulted in progressive decline in levels of AR, PSA, and PSM mRNA expression, but could not reverse its aggressive growth pattern. CL1 and CL2 cells were capable of potentiating the growth of endothelial and bone marrow stromal cells in co-culture experiments, and acquired significant resistance to radiation and to anti-cancer cytotoxic agents (Taxol, Vinblastine, and Etoposide). In contrast to the poorly tumorigenic parental LNCaP cells, CL1 and CL2 lines proved highly tumorigenic, exhibiting invasive and metastatic characteristics in intact and castrated mice or in female mice within a short period of 3-4 weeks. No growth supplements (e.g. Matrigel) were needed. When transfected with the green fluorescence protein (GFP) gene and transplanted orthotopically in the prostate, extensive metastatic disease from the primary CL tumor could be identified in bone, lymph nodes, lung, liver, spleen, kidney and brain. Quantitative RT-PCR analysis revealed a markedly distinct molecular expression profile in the CL lines: over-expression of b-FGF, IL-6, IL-8, VEGF, TGF-β, EGF-R, caveolin, and bcl-2 mRNAs and a markedly down-regulated E-cadherin, p-53, and PTEN. Early administration of hormonal therapy following failure of first line treatment is associated with a profound clonal selection of aggressive AI variants such as CL1 and CL2 lines. These tumor lines with their parental counterparts can serve as valuable tools for studying the cellular and molecular mechanisms of CaP progression and metastasis under hormonal therapy. CL1 and CL2 offer an unique and reproducible model for the evaluation of drug sensitivity and for other therapeutic modalities for advanced prostate cancer.

Introduction

Androgen deprivation forms the basis of endocrine therapy for the majority of patients with advanced prostate cancer (1). Unfortunately, most men eventually develop hormone refractory disease despite maximal androgen ablation (2). The mechanisms for tumor progression to hormone independence remain mostly unknown. Whether CaP progression to an androgen-independent (AI) stage involves an adaptive mechanism; or the existence and outgrowth of a pre-existing AI variant(s) which had been part of the original heterogeneous tumor population remains to be established. Nevertheless, it appears that AI variants have adapted a "detour" growth pathway(s), which allows the cells to by-pass the requirement for androgen as a primary growth factor. Elucidation of the factors and mechanisms that dictate this adaptive survival response to an androgen-free signaling growth pathways can lead to a more rational strategy for the management of HRPC including the possibility of preventing AI cell overgrowth.

Comparison between non-treated metastatic CaP and primary or recurrent tumors that had been exposed to long-term androgen deprivation therapy shows very similar losses or gains of chromosomal alterations (3). This finding implies that minor genetic differences are more likely to be involved in development of the AI phenotype. It is also suggested that modified functions or expressions of genes in CaP may be largely responsible for cell survival in the absence of androgen, as well as the malignant phenotype. Androgen receptor mutations have been identified in HRPC tumors and were felt to contribute to the loss of ligand specificity as well as activation of ligand-free growth response (4-6). In addition, loss of androgen dependence is believed to be associated with an increase in tumorigenic stem cells and resistance to cell death genes (7). The recent use of gene transfer technology further supports these mechanisms, and demonstrates that certain molecular changes in CaP render hormonal escape, activation of ligand-independent growth, resistance to apoptosis, and enhancement of tumorigenicity (8-10). In this study, we have created a model system enabled the selection of hormone refractory variants from an AD CaP

culture cell line via androgen deprivation treatment. Our aim was to isolate AI variants form AD CaP culture cell lines without exposure to transfectants or supplemental modulation, thus mimicking the characteristics of clinically occurring HRPC tumors. These tumors usually exhibit a more aggressive phenotype that is resistant to conventional therapy when compared to the corresponding parental AD tumors. Using the existing in-vitro cell line model, LNCaP; which is an androgen-dependent CaP cell line expressing PSA, PSM, and AR and has a slow growth pattern in mice (11-14), we were able to perform kinetic studies to characterize the changes in cell behavior and the molecular modulations that are associated with transition from AD to the AI phenotype.

Materials and Methods

In-Vitro Androgen Deprivation Treatment. The human prostate cancer cell line, LNCaP provided by American Type Culture Collection (Rockville, MD) was maintained in medium supplemented with 10% fetal bovine serum and antibiotics (penicillin -50 IU/ml; streptomycin-50 μg/ml). Androgen deprivation treatment was carried out by removing medium from LNCaP cultures (80%-90% confluence) and replacing with serum-free RPMI 1640 medium. Cells were rinsed twice with serum-free medium for 5 minutes each and then further incubated in serum-free medium at 37 °C for 15 minutes. After medium was removed, culture medium was replaced with RPMI1640 supplemented with 10% charcoal-stripped serum and antibiotics (15). LNCaP variants selected by androgen withdrawal and maintained in charcoal-stripped serum-supplemented RPMI media were designated CL1. After six weeks of culture selection, CL1 cells were returned to regular serum supplemented medium and designated CL2. Experiments performed in this paper using CL1 were always carried out in culture medium supplemented with

charcoal-stripped serum whereas both parental LNCaP and CL2 were kept in medium supplemented with regular serum.

Quantitative Reverse Transcriptase-Polymerase Chain Reaction (RT-PCR). Total RNA was extracted from LNCaP, CL1, and CL2 during and after androgen deprivation, by acid guanidine isothiocyanate-phenol-chloroform extraction. The amounts of diluted RNA samples which express equivalent signal intensity of β-actin were used to perform PCR reaction for other molecules of interest. Messenger RNA was reverse transcribed into cDNA by incubating titrated RNA with AMV reverse transcriptase, primer oligo (dT), dNTP, and RNAse inhibitor at 42°C for 1 hour. One μl of each cDNA sample was amplified utilizing PCR in a total volume of 25 μl, containing 30 ng [^{32}P]-5'-oligonucleotide primer (kinased with bacteriophage T4- polynucleotide kinase and [^{32}P]-γ-ATP), 100 ng 3'-oligonucleotide primer, 2.5 μl modified 10X PCR buffer (25 mM Tris, pH 8.0, 1.5 mM $MgCl_2$, 0.25 mM dATP, dTTP, dCTP, dGTP, and 100 μg/ml bovine serum albumin), 1.25 U Taq polymerase, and autoclaved double distilled water to fill the volume to 25 μl. The PCR mixture was amplified for 25 cycles in a DNA Thermocycler (Perkin-Elmer, Norwalk, CT). Each cycle consisted of denaturation at 94°C for one minute and annealing/extension at 65°C for 2 minutes. The ^{32}P-labeled PCR products were visualized directly by acrylamide gel electrophoresis and autoradiography, and then quantitated by band excisions and subsequent scintillation counting. The signal intensity of each amplified product was calibrated to its corresponding β-actin mRNA expression as an internal control for quantitation of expression levels. The quantitative analysis was further elucidated by a serial dilution of mRNA (1:3, 1:10, 1:30 and 1:300) and co-amplification of β-actin and other molecule of interest. The following oligonucleotide primer pair sequences were used:

β-Actin-5' CAACTCCATCATGAAGTGTGAC, 3'CTCGCGTTCATGAGGCACACC (184 bp); PSA-5'TGTCTCGGATCCTGGGAGGCTG, 3' CTCAGGAATTCGCCACGA (195 bp); AR-

5'CAAGCTCCTG GACTCCTGGCA, 3'TAGATGGGCTTGACTTTCCC (140 bp); PSM-5' CCAAGTTCAGTGAGA GACTC, 3' GCTACTTCACTCAAAGTCTC (308 bp); IL-8-5CATACTCCAAACCTTTCCAC, 3'TCTTCAAAAACTTCTCCACAA; VEGF-5' ATGCGGATCAAACCTCACC, 3'ATCTGGTTCC CGAAACCCTG (159 bp); bFGF-5' CCCAAGCGGCTGTACTGCAA, 3' AGCTCTTAGCAGACATTGG (383 bp); IL-6-5'ATGTAGCCGCCCCACACAGA, 3'CATCCATCTTTTTCAGCCAT (171 bp); TGFβ1-5' GACTTCCGCAAGGACCTCGGC, 3' GCGCACGATCATGTTGGACAG (250 bp);TGF-β2-5'CCTGT CTACCTGCAGCACACTCGA, 3' GGCGGCATGTCTATTTTGTAAACCTCC (290 bp); TGF β -R-5' CGACA TGATA GTCAC TGACA ACAAC, 3' CTGAG AAGAT GATGT TGTCA TTGCA (350 bp); EGFF-R-5' CTTCTTGCAGCGATACAGCTC,3' ATGCTCCAATAAATTCACTGC (441 bp); BCL- 2-5'CTTTGAGTTCGGTGGGGTCATGTG, 3' TGACTTCACTTGTGGCCCAG ATAG (318 bp); E-cadherin- 5' CTGAAGTGACTCGTAACGAC, 3' CATGTCTGCCAGCTTCTTGAAG (286 bp); P53-5'TGGTACAGTCAGAGCCAACC, 3' AGCAGTCACAGCACATGACG (201bp); PTEN- 5' GGACG-AACTGGTGTAATGATATG, 3' TCTACTGTTTTTGTGAAGTACAGC (671 bp); Caveolin-5'AGAAG CAAGTGTACGAC, 3' AGGAAGCTCTTAATGCA (300 bp); c-myc-5' AAGTCCTGCGCCTCG CAAGA, 3' AGGTTTGCTGTGGCCTCCAG (255 bp); HER-2/neu- 5' TAGACACCAACCGCTCTCGG, 3' CACTGCTCATGGCAGCAGTC (168 bp); P27-5' TGCAGGAACCTCTTCGG, 3'TTGCAGGTCG CTTCCTTAT (385 bp).

Proliferation Assay, Growth Expansion, Cell Cycle Analysis, and Colony-Forming Assay. Proliferation of assay was carried out by ^{3}H-thymidine incorporation. Briefly, Cells were seeded on a 24-well plate in triplicate at the concentration of 3 x 10^{4}/ml of culture medium. Cell were incubated at 37°C for 48 hr and then pulsed with 1 μCi of ^{3}H-thymidine for 24 hr. The incorporated ^{3}H-thymidine was measured by scintillation counting with a β counter. Growth

curve of cell lines were established by seeding 1 x 10^4 cells /3 ml/well in 6- well plates in triplicate. A total of 10 culture sets were plated. Cell counts were performed in one set every 6 hr until the last set of cells nearly reached confluence. Cell cycle analysis was carried out by propidium iodide staining as previously described (16). Washed cell pellets ($1x10^6$) were resuspended in 1 ml of the hypotonic DNA staining buffer. Cells were kept at 4°C, and protected from light for 30 min before acquisition on the flow cytometer. Colony-forming efficiency of cell lines was measured by seeding cells at a concentration of 100, 500, and 1000 cells respectively in 100 mm Petri culture dishes. After incubation for 7 days, cells were fixed with 80 % alcohol for 30 min and stained with 1% crystal violet solution in PBS. The visualized cell colonies were counted and compared.

Co-Culture Experiments. Parental LNCaP cells or CL variants (upper compartment - 2 x 10^4 /200 µl) were co-cultured with human umbilical endothelial cells (provided by Dr. Pauli Benedicht, Conell University, Ithaca, NY) or human bone marrow stromal cells (provided by Dr. Judy Gasson, UCLA School of Medicine, Los Angeles, CA) (lower compartment- 2 x 10^4 /600 µl) in Transwell culture plates (Costa, Pleasanton, CA) using a dish insert with a porous bottom permitting free exchange of the released factors between the lower and upper compartments. Following a 48 hr incubation at 37 °C, the inner wells were removed, and the cells in the bottom wells were pulsed with 1µCi of tritiated ^{3}H-thymidine for an additional 12 hrs. After three washes, cell were lysed with 0.5 % SDS, and the lysates were placed in scintillation cocktail and measured in a β-counter.

Radiation and Drug Sensitivity Assay. The response of the parental LNCaP cells and their AI variants to radiation treatment was assayed in 24-well plates. Aliquots of 3 x 10^4 cells were seeded in triplicate. Each cell type was seeded in five individual plates in order to deliver

different dose of radiation. Following cell adherence, cells were irradiated with 0, 2, 4, 6, and 8 Gy, respectively. Fresh culture medium was replaced and cells were continually incubated for a 48-hr period prior to pulsing with 1 μCi of tritiated ^{3}H-thymidine.

To test the sensitivity of cells to a variety of chemotherapeutic agents, aliquots of 3 x 10^4 cells were plated in triplicate 24-well culture plates. Following cell adherence, culture medium with or without a cytotoxic agent was added. Serial twofold dilutions were performed to span the effective dose range for each drug as described (17). The drugs tested included Vinblastin (vinca alkaloids-VBL) (Eli Lilly Co., Indianapolis, IN), Taxol (taxanes-TAX) (Mead Johnson, Princeton, NJ), and etoposide (topoisomerase II inhibitors –VP-16)(Bristol Laboratories, Princeton, NJ). Following a 48 hr incubation at 37 °C, cells were pulsed with 1μCi of tritiated ^{3}H-thymidine for an additional 12 hrs before harvesting. The sensitivity of cells to radiation and drug treatment were expressed by percent of growth inhibition which was calculated by [(a-b)/a] x 100%, where a = ^{3}H-thymidine uptake by cells without radiation or drug treatment and b = ^{3}H-thymidine uptake by surviving cells with radiation or drug treatment.

Animal studies. Male or female 6-8 week-old SCID (C.B.-17 scid/scid) mice were obtained from the breeding program at UCLA. All animals were anesthetized with methoxyflurane before inoculation of cancer cells. For s.c. tumor growth, 1x10^6 cells were resuspended in 100 μl of RPMI1640 medium without other supplements and injected via a 27-gauge needle into the subcutaneous tissue of the flanks of SCID mice. Tumor growth was measured twice weekly, and the tumor size was calculated by the formula cube root of L x W x H (mm) giving the mean diameter of tumor size (18). For intraprostatic tumor growth, 5 x 10^4 cells in 5 μl of RPMI 1640 were injected under the prostatic capsule via a 30-gauge needle. To characterize tumor growth in the bone, intratibial injection was performed by delivering 4 x 10^4 cells in 2 μl of RPMI 1640

medium. The invasiveness of tumors was examined grossly and histologically for the presence of tumor mass. Bone scan was performed by a certified nuclear medicine physician.

Green fluorescent protein (GFP) gene transfer and analysis of metastases. pCEP4 plasmid vector was purchased from Invitrogen (Carlsbad, CA). The GFP gene driven by CMV promoter was inserted into pCEP4 which contains hygromycin resistance gene. Gene transfection of CL1 and CL2 cells was carried out by electroporation as described previously (19). Drug resistant colonies were selected and expanded with 200 μg/ml hygromycin (Sigma, St. Louis, MO). The established CL-GFP cell lines used for animal study contained 99.9 % GFP expression cells as determined by flow cytometry. Four to 5 weeks after orthotopic injection, the primary tumor and all major organs were examined for the evidence of metastatic disease. Fresh samples were either sliced at 1 mm thickness without treatment and observed under fluorescence microscopy or snap frozen in isopentane and dry ice, and embedded in OCT for cryostat sections at 5 μm.

Results

Clonal Selection and Expansion of Hormone Refractory Prostate Cancer by Androgen Deprivation Treatment. When growth condition of LNCaP cell cultures was changed to medium supplemented with charcoal-stripped serum, a large fraction of cells underwent apoptosis and gradually detached from the culture flasks. Initially, no growth activity could be detected in the cultures. However, a few small epithelial-like clones that strongly adhered to the plastic surface were identified in the second week of culture and continued to rapidly expand eventually becoming a stable AI cell line. This cell line was designed CL1 (Figure 1). Following propagation of CL1 in culture for six weeks, the culture condition was changed back to regular-serum containing medium. No changes in morphology or growth profile were observed

compared to the CL1 cells. The cell culture which continued to propagate in regular medium was designated CL2.

Transcriptional Regulation of Prostate Specific Genes in Response to Androgen Deprivation Treatment. When LNCaP cell cultures were subjected to androgen withdrawal, transcriptional activity of AR, PSA, and PSM genes were down-regulated within the first 24 hr. However, a return of AR and PSM mRNA expression levels were detected at 72 hr with a steady increase of AR mRNA expression over several weeks accompanied by a progressive decline in PSA mRNA (Figure 2). Prostate specific membrane antigen however was only slightly up-regulated. Prolonged androgen deprivation treatment of LNCaP cells resulted in the establishment of CL1, an AI cell line, that no longer can be reverted to androgen sensitivity upon changing culture conditions back to regular medium. Thus, CL1 or CL2 could not be reverted to a parental LNCaP line. However, even though a return of PSA mRNA was detected within the first 6 hr after the return of CL1 to regular medium, a rapidly diminished PSA mRNA expression was detected in the 72 hr sample which accompanied a low expression level of AR and PSM mRNAs (Figure 2). A similar low profile of androgen regulated gene expression was also observed in high passage CL1 line (Figure 11).

Differential Growth Characteristics in CL Cells Compared to Parental LNCaP Cells. Growth profiles of CL1 and CL2 cells were characterized by cell cycle analysis, ^{3}H-thymidine incorporation, growth expansion, and plating/colonization efficiency and compared to parental LNCaP cells. The results showed that the proportion of cells in synthesis phase (S phase) increased two to three-fold in both CL1 (33.62%) and CL2 (50.44%) as compared to LNCaP cells (15.37%) (Figure 3). These results also corresponded to a five to seven fold increase in ^{3}H-thymidine uptake in CL lines as compared to LNCaP cells (Figure 4). In addition, growth

expansion curves of CL lines were compared to parental LNCaP cells revealing a ten-fold growth expansion at 60 hrs in CL lines in contrast to a two-fold expansion in parental LNCaP cells (Figure 4). When cell density was increased, the doubling time of CL cells was decreased from 30 hr to 12 hr, whereas the doubling time of LNCaP cells was maintained at 48 hrs in the assays. The colony forming efficiency was also compared among the three cell lines. Based on colony counts, there was an approximately 460 and 530- fold increase determined in CL1 and CL2 lines respectively when compared to parental LNCaP cells (Figure 5).

Enhanced Interaction of CL Cells to Human Endothelial Cell and Bone Marrow Stromal Cells. Prostate cancer progression is characterized as local invasion, angiogenesis, and metastasises. Bone is a primary metastatic site in CaP. To assay whether AI CL lines can stimulate the growth of endothelial cells and bone marrow stromal cells to a greater extent than their AD counterpart; the growth stimulation of human endothelial cells and bone marrow stromal cells by parental LNCaP cells and CL cells was measured in Transwell co-culture plate (see Materials and Methods). As compared to parental LNCaP, both CL lines exhibited an approximately two-fold increase in growth stimulation of endothelial and bone marrow stromal cells (Figure 6A, 6B). Similar results were detected when parental LNCaP cells were seeded with two-fold cell numbers in order to compensate for its' slow-growing nature (data not shown).

Treatment Resistance of CL Cells to Radiation and Chemotherapeutic Agents. To evaluate the sensitivity to radiation and to phamacotherapy CL lines, growth activity was analyzed. The antiproliferative and cytotoxic responses to radiation and chemotherapy were assayed by ^{3}H-thymidine incorporation and percent growth inhibition. When compared to LNCaP cells, minimal growth inhibition (5 –10%) was detected in both CL1 and CL2 with maximal treatment doses of eight Gy. In contrast, 58% growth inhibition was determined in

LNCaP cells irradiated with a minimal treatment dose of 2Gy (Figure 7). Similarly, enhanced chemoresistance was detected in both CL lines when compared to LNCaP cells. All three drugs tested, Vinblastine (Figure 8A), Taxol (Figure 8B), and Etoposide (Figure 8C) had achieved 70-85% growth inhibition of LNCaP cells using the lowest treatment dose (0.625 nM, 0.625 nM, 0.625 μM), yet equivalent growth suppression was not achievable in CL lines even with the highest treatment doses of Vinblastine (20 nM) and Etoposide (20μM). However, with Taxol, 80 % growth inhibition was achieved with dose of 10 nM on both CL lines.

Invasive and Metastatic Behavior of CL Lines in SCID Mice. LNCaP exhibited minimal tumorigenicity in SCID unless mixed with Matrigel or bone stromal cells (20). In contrast, both CL1 and CL2 cells rapidly induced tumor formation (palpable tumor within two weeks) in SCID mice via subcutaneous, intraprostatic or intratibial injection, with a tumor take rate of 100% in both male and female mice or castrated male mice (5/5 in each group). Notably, CL1 tumor exhibited a tendency to grow slower than CL2 (Figure 9). All mice receiving intraprostatic injection (5 weeks), demonstrated an aggressive local invasion of adjacent organs specifically major lymphadenopathy with tumor spread to rectum, bladder, seminal vesicles, vertebral column, and distal retroperitoneal lymph nodes (Figure 10A). In addition, following intraprostatic injection of CL cells transfected with *Aequorea victoria* jellyfish GFP gene, metastatic disease was identified in bone, lymph nodes, lung, liver, spleen, kidney and brain (Figure 11 A-H) (21). Intratibial injections of CL cells led to aggressive local growth with bulky lesions demonstrated by plain radiography (Figure 10B, 10C). Pathological evaluation confirmed aggressive tumor growth with complete invasion and destruction of bone tissue by tumor around the injection site, in addition to retroperitoneal lymph nodes metastasis (22,23). Retroperitoneal lymph node metastases were found in 100% of mice with either intraprostatic or intratibial tumors, whereas no metastases were found in mice with subcutaneous tumors.

Molecular Determinants for Malignant Behavior of CL Variants. When compared to LNCaP cells over-expression of the autocrine growth factors and angiogenic factors b-FGF, IL-6, IL-8, VEGF, TGF- β1, TGF-β2, TGFβ-R, and EGF-R mRNAs were detected in CL1 cells, whereas only IL-8, VEGF, and b-FGF but not TGFβ1/β2, TGFβ-R, or EGFR mRNA expressions were up-regulated in CL2 (Figure 12). Loss of E-cadherin mRNA expression was detected in both CL1 and CL2 cells. In addition, diminished levels of p53 and PTEN with augmented BCL-2 mRNA expression were determined in both CL cells when compared to LNCaP cells. Enhanced caveolin mRNA expression was only detected in CL1 but not in CL2 cells whereas HER-2/neu mRNA expression was slightly upregulated in both CL cells when compared to LNCaP cells. Similar mRNA level of c-myc and p27 was detected in all three cell lines (Figure 11).

Discussion

In this report, we demonstrate that androgen deprivation in tissue culture can lead to the outgrowth of highly aggressive AI variants. When compared to AD parental cells with low tumorigenicity, CL variants demonstrated both invasive and metastatic potential in SCID mice within a very short time period without any additional supplements or gene transfer manipulations. This points out to the emergence of an unique clone(s) with a malignant genotype established in CL cell lines. At the present time, the mechanisms underlying the development of metastatic and androgen independent phenotypes in prostate cancer are unknown. Therefore, our model can provide clues for further identifying the cellular and molecular mechanisms responsible for hormonal escape and CaP progression.

Our data suggests that androgen deprivation is a contributing factor in the selection and growth of a more aggressive cell population over time. Whether CL1 was derived from the

selective outgrowth of a low frequency AI stem cells present in the parental LNCaP line, or from an adaptive modification of a low frequency AD stem cells to androgen deprivation, remains to be established. Replacement of androgen in CL1 culture did not lead to reversal to AD phenotype since CL2 expressed malignant features in female mice, indicating a selection of a pure AI population. AI variants are probably utilizing alternative growth pathways manifested by over-expression of growth factor and growth factor receptor mRNAs in CL1. Enhanced growth factor production may render the ability of CL to bypass the requirement for androgen. This finding further supports the hypothesis that paracrine growth factors in normal prostate or early stages of AD tumors may switch to autocrine stimulation with tumor progression to the AI phenotype (24-27). In addition to their growth effects, many growth factors also contribute to motility, invasion, and metastatic spread (28). The high levels of VEGF, IL-8 and bFGF mRNA expression by both CL lines may explain their aggressive behavior in animals as well as the growth stimulation of endothelial cells and bone marrow stromal cells observed in co-culture experiments. Several LNCaP sublines with AI phenotypes have been isolated and characterized (20, 29-32). Bone stromal cells support the induction of tumorigenicity and the selection of invasive and metastatic phenotype of LNCaP subclones in animals indicating that fibroblast derived growth factors have an important role in modulation of both genotype and phenotype of CaP (25). Likewise, overexpression of endogenous growth factors in CL lines including angiogenic factors are likely to be responsible for the aggressive growth and metastasis of the AI tumor grown in androgen deficient environment. Discrete growth mechanisms by growth factors other than androgen have been previously suggested (33).

Changes in the apoptotic potential of tumor cells may also be responsible for the phenomenon of hormonal escape. Overexpression of bcl-2 (34-36) accompanied with diminished levels of p53 (36-38) and PTEN mRNA expression in CL lines might explain the resistance to apoptosis with its rapid growth, radiation insensitivity and chemoresistance (39,

40). Enhanced expression of caveolin has been associated with androgen-resistance and prostate cancer progression (10). We however observed that although an up-regulated caveolin mRNA expression was found in CL1, the expression level in CL2 (grown in the presence androgen but has AI phenotype) diminished to the equivalent level seen in parental LNCaP cells, yet it did not affect its aggressive behavior in female mice or castrated mice. We thus believe that caveolin is an androgen-repressed gene but may not be directly associated with tumor progression in the CL line. Distinct genetic basis in CaP progression and development of AI growth has been postulated (41). IL-6-mediated up-regulation of AR activity in a ligand-independent manner in CaP patients has been suggested (42). Down regulation of TGF-β, IL-6 and EGFR mRNA expression were also seen in CL2 as compared to CL1. We believe that this may reflect the cell response to the restoration of exogenous androgen and to the growth factors in CL2 culture medium. Abnormal expression of E-cadherin molecules in CaP correlates with Gleason score and the extent of bone metastasis (43). Loss of E-cadherin mRNA expression in both CL1 and CL2 may therefore further underlie the observed malignant phenotype.

Several AI mouse models of metastatic human prostate cancer have been developed so far. Most of them have been established via natural in vivo selection following castration (20, 44, 45). Our unique CL animal model, however, is the first AI tumor model that was derived from in-vitro androgen deprivation selection. Growth characteristics of CL1 and CL2 lines resemble the tumor growth kinetics in patients with advanced CaP who progress during androgen withdrawal (33). With no stromal or mouse cells involved, and with the availability of a parental AD LNCaP counterpart, CL1 and CL2 lines offer a unique model for cellular and molecular dissection of the mechanism of CaP progression under androgen deprivation therapy. Our current findings suggest that new therapeutic strategies for the treatment of HRPC should be directed to manipulating the autocrine, paracrine, and angiogenic growth factors as well as reactivating the sensitivity to cell death pathways.

References

1. Stamey, T. A., McNeal, J. E. Adenocarcinoma of Prostate. In: Campbell's Urology, 6th ed. Walsh P, Retil AB, Stamey TA, Vaughan ED, editors. pp 1159-1221, Philadelphia: W.B. Saunders, , 1992.
2. Leewansangtong, S., and Soontrapa, S. Hormonal ablation therapy for metastatic prostatic carcinoma: a review. J. Med. Asso.Thailand 82:192-205, 1999.
3. Cher, M. L., Bova, G. S., Moore, D. H., Small, E. J., Carroll, P. R., Pin, S. S., Epstein, J. I., Isaacs, W. B., and Jensen, R. H. Genetic alterations in untreated metastases and androgen-independent prostate cancer detected by comparative genomic hybridization and allelotyping. Cancer Res., 56: 3091-3102, 1996.
4. Trapman, J., and Brinkmann, A. O. The androgen receptor in prostate cancer. Pathol Res. Prac., 192: 752-760, 1996.
5. Tilley, W. D., Buchanan, G., Hickey, T. E., and Bentel, J. M. Mutations in the androgen receptor gene are associated with progression of human prostate cancer to androgen independence. Clin. Cancer Res., 2: 277-285, 1996.
6. Sadar, M. D. Androgen-independent induction of prostate-specific antigen gene expression Via cross-talk between the androgen receptor and protein kinase A signal transduction pathways. J. Biol.Chem., 274: 7777-7783, 1999.
7. Rennie, P. S., Bruchovsky, N., and Coldman, A. J. Loss of androgen dependence is associated with an increase in tumorigenic stem cells and resistance to cell-death genes. J. Steroid Biochem. Mol. Biol., 37: 843-847, 1990.
8. Chen, Y., Martinez, L. A., LaCava, M., Coghlan, L., and Conti, C. J. Increased cell growth and tumorigenicity in human prostate LNCaP cells by overexpression to cyclin D1. Oncogene 16: 1913-20, 1998.

9. Craft, N., Shostak, Y., Carey. M, and Sawyers, C. L. A mechanism for hormone-independent Prostate cancer through modulation of androgen receptor signaling by the HER-2/neu tyrosine kinase, Nature Med., 5: 280-285, 1999.

10. Nasu, Y., Timme, T. L., Yang, G., Bangma, C. H., Li, L., Ren, C., Park, S. H., DeLeon, M., Wang, J., and Thompson, T. C. Suppression of caveolin expression induces androgen sensitivity in metastatic androgen-insensitive mouse prostate cancer cells. Nature Med., 4: 1062-4,1998.

11. Montgomery, B. T,. Young, C. Y,. Bilhartz, D., Andrews, P. E,. Prescott, J. L., Thompson, N. F., and Tindall, D. J. Hormonal regulation of prostate-specific antigen (PSA) glycoprotein in the human prostatic adenocarcinoma cell line, LNCaP. Prostate 21: 63-73, 1992.

12. Israeli, R. S., Powell, C. T., Corr, J. G., Fair, W. R., and Heston, W. D. Expression of the prostate- specific membrane antigen. Cancer Res., 54:1807- 1811, 1994.

13. Veldscholte, J., Ris-Stalpers, C., Kuiper, G. G., Jenster, G., Berrevoets, C., Claassen, E., van Rooij, H. C., Trapman, J., Brinkmann, A. O., and Mulder, E. A mutation in the ligand binding domain of the androgen receptor of human LNCaP cells affects steroid binding characteristics and response to anti-androgens. Biochem.Biophy. Res. Commu., 173: 534-540, 1990.

14. Lim, D. J., Liu, X. L., Sutkowski, D. M., Braun, E. J., Lee, C., and Kozlowski, J. M. Growth of an androgen-sensitive human prostate cancer cell line, LNCaP, in nude mice. Prostate 22:109-118, 1993.

15. Aakvaag, A., Utaaker, E., Thorsen, T., Lea, O. A., and Lahooti, H. Growth control of human mammary cancer cells (MCF-7 cells) in culture: effect of estradiol and growth factors in serum-containing medium. Cancer Res., 50: 7806-7810, 1990.

16. Krishan, A. Rapid flow cytofluorometric analysis of mammalian cell cycle by propidium iodide staining. J. Cell Biol., 66:188-193, 1979.

17. Pegram, M. D., Finn, R. S., Arzoo, K., Beryt, M., Pietras, R. J., and Slamon, D. J. The effect of HER-2/neu overexpression on chemotherapeutic drug sensitivity in human breast and ovarian cancer cells. Oncogene **15,** 537-547 (1997).

18. Twentyman, P. R., Kallman, R. F., and Brown, JM. The effect of time between X-irradiation and chemotherapy on the growth of three solid mouse tumors--II. Cyclophosphamide. Int. J. Radi. Oncol. Biol. Phy., 5:1425-1427, 1979.

19. Pang, S., Dannull, J., Kaboo, R., Xie, Y., Tso, C-L., Michel, K., deKernion, JB., and Belldegrun, AS. Identification of a positive regulatory element responsible for tissue-specific expression of prostate-specific antigen. Cancer Res., 57:495-499, 1997.

20. Wu, H. C., Hsieh, J. T., Gleave, M. E., Brown, N. M., Pathak, S., and Chung, LW. Derivation of androgen-independent human LNCaP prostatic cancer cell sublines: role of bone stromal cells. Intl. J. Cancer 57: 406-412, 1994.

21. Yang M., Jiang, P., Sun, F. X., Hasegawa, S., Baranov, E., Chishima, T., Shimada, H., Moossa, A, R.., Hoffman, R. M. A fluorescent orthotopic bone metastasis model of human prostate cancer. Cancer Res., 59: 781-786, 1999.

22. Soos, G., Jones, R. F., Haas, G. P., and Wang, C. Y. Comparative intraosseal growth of human prostate cancer cell lines LNCaP and PC-3 in the nude mouse. Anticancer Res., 17: 4253-4258, 1997.

23. Rabbani, S. A., Gladu, J., Harakidas, P., Jamison, B., Goltzman, D. Over-production of parathyroid hormone-related peptide results in increased osteolytic skeletal metastasis by prostate cancer cells in vivo. Intl J Cancer 80: 257-64, 1999.

24. Culig, Z., Hobisch, A., Cronauer, M. V., Radmayr, C., Hittmair, A., Zhang, J., Thurnher, M., Bartsch, G., and Klocker, H. Regulation of prostatic growth and function by peptide growth factors. Prostate 28: 392-405, 1996.

25. Russell, P. J., Bennett, S., and Stricker, P. Growth factor involvement in progression of prostate cancer. Clin. Chem., 44: 705-723, 1998.

26. Scher, H. I., Sarkis, A., Reuter, V., Cohen, D., Netto, G., Petrylak, D., Lianes, P., Fuks, Z., Mendelsohn, J., and Cordon-Cardo, C. Changing pattern of expression of the epidermal growth factor receptor and transforming growth factor alpha in the progression of prostatic neoplasms. Clin. Cancer Res., 1: 545-550, 1995.

27. MacDonald, A., and Habib, F. K. Divergent responses to epidermal growth factor in hormone sensitive and insensitive human prostate cancer cell lines. British J. Cancer 65:177-82, 1992.

28. Szabo, S., and Sandor, Z. The diagnostic and prognostic value of tumor angiogenesis. Eur. J. Surgery. Supplement 582, 99-103 (1998).

29. Pousette, A, Carlström, K, Henriksson, P, Grande, M, and Stege, R. Use of a hormone-sensitive (LNCaP) and a hormone-resistant (LNCaP-r) cell line in prostate cancer research. Prostate 31: 198-203, 1997.

30. Platica, M., Verma, R.S., Macera, M. J., and Platica, O. LNCaP-OM, a new androgen-resistant prostate cancer subline. In Vitro Cellu. Devel., mental Biolo. Animal 33:147-149, 1997.

31. Joly-Pharaboz, M.,O., Soave, M. C., Nicolas, B., Mebarki, F., Renaud, M., Foury, O., Morel, Y., and Andre, J. G. Androgens inhibit the proliferation of a variant of the human prostate cancer cell line LNCaP. J. Steroid Biochem. Mol. Biol., 55: 67-76, 1995.

32. van Steenbrugge, G. J., van Uffelen, C. J., Bolt, J., and Schröder, F. H. The human prostatic cancer cell line LNCaP and its derived sublines: an in vitro model for the study of androgen sensitivity. J. Steroid Biochem. Mol. Biol., 40:207-214, 1991.

33. Koivisto, P., Visakorpi, T., Rantala, I., and Isola, J. Increased cell proliferation activity and decreased cell death are associated with the emergence of hormone-refractory recurrent prostate cancer. J. Pathol., 183:51-56, 1997.

34. Gao, M., Ossowski, L., and Ferrari, A. C. Activation of Rb and decline in androgen receptor protein precede retinoic acid-induced apoptosis in androgen-dependent LNCaP cells and their androgen-independent derivative. J. Cellu. Physiol., 179, 336-346, 1999.

35. McDonnell, T. J., Troncoso, P., Brisbay, S. M., Logothetis, C., Chung, L. W., Hsieh, J. T., Tu, S. M., and Campbell, M. L. Expression of the proto-oncogene bcl-2 in the prostate and its association with emergence of androgen-independent prostate cancer. Cancer Res., 52: 6940-694, 1992.

36. DiPaola, R. S., and Aisner, J. Overcoming bcl-2- and p53-mediated resistance in prostate cancer. Semin. Oncolo., 26 (1 Suppl 2):112-116, 1999.

37. McDonnell, T. J., Navone, N. M., Troncoso, P., Pisters, L. L., Conti, C., von Eschenbach, A. C., Brisbay, S., and Logothetis, C. J. Expression of bcl-2 oncoprotein and p53 protein accumulation in bone marrow metastases of androgen independent prostate cancer. J. Urolo., 157: 569-574, 1997.

38. Cheng, L., Sebo, T. J., Cheville, J. C., Pisansky, T. M., Slezak, J., Bergstralh, E. J., Pacelli, A., Neumann, R. M., Zincke, H., and Bostwick, D. G. p53 protein overexpression is associated with increased cell proliferation in patients with locally recurrent prostate carcinoma after radiation therapy. Cancer 85:1293-1299, 1999.

39. Wu, X., Senechal, K., Neshat, M. S., Whang, Y. E., and Sawyers, CL. The PTEN/MMAC1 tumor suppressor phosphatase functions as a negative regulator of the phosphoinositide 3-kinase/Akt pathway. Pro. Natl. Acad. Sci., (USA) 95: 15587-15591, 1998.

40. Gao, M., Ossowski, L., and Ferrari, AC. Activation of Rb and decline in androgen receptor protein precede retinoic acid-induced apoptosis in androgen-dependent LNCaP cells and their androgen-independent derivative. J Cell Physiol., 179:336-346, 1999.

41. Visakorpi, T.,; Kallioniemi, A. H., Syvänen, A. C., Hyytinen, E. R., Karhu, R., Tammela, T., Isola, J. J., Kallioniemi, OP. Genetic changes in primary and recurrent prostate cancer by Comparative genomic hybridization. Cancer Res., 55: 342-347, 1995.

42. Hobisch, A., Eder, I. E., Putz, T., Horninger, W., Bartsch, G., Klocker, H., and Culig, Z. Interleukin-6 regulates prostate-specific protein expression in prostate carcinoma cells by activation of the androgen receptor. Cancer Res., 58: 4640-4645, 1998.

43. Richmond, P. J., Karayiannakis, A. J., Nagafuchi, A., Kaisary, A.V., Pignatelli, M. Aberrent E- cadherin and alpha-catenin expression in prostate cancer: correlation with patient survival. Cancer Res., 57: 3189-3193, 1997.

44. Klein, K. A., Reiter, R. E., Redula, J., Moradi, H., Zhu, X. L., Brothman, A. R., Lamb, D. J., Marcelli, M., Belldegrun, A., Witte, O. N, and Sawyers, C. L. Progression of metastatic human prostate cancer to androgen independence in immunodeficient SCID mice. Nature Med., 3: 402-408, 1997.

45. van Weerden, W. M,. de Ridder, C. M., Verdaasdonk, C. L., Romijn, J. C,. van der Kwast, T. H., Schroder, F. H,. and van Steenbrugge, G. J. Development of seven new human prostate tumor xenograft models and their histopathological characterization. Amer. J. Pathol., 149:1055-1062, 1996.

Legends to Figures

Figure 1. Clonal selection and expansion by androgen deprivation treatment of LNCaP cells in culture. Light microscopic pictures showing A, parental LNCaP cell prior to androgen deprivation (X100); B-D, outgrowth of new colonies during the second week of the androgen deprivation treatment (X100); E, stable androgen-independent cell line derived from LNCaP designed CL1 (six weeks after androgen deprivation) (X400); F, CL2 cell line generated by growing CL1 cells in the presence of androgen-containing medium (5 weeks after re-exposure to androgen) (x100)

Figure 2. Quantitative RT-PCR analysis for PSA, PSM and AR mRNA expression in LNCaP cells under androgen deprivation between and following androgen restoration. RNAs were extracted from LNCaP cells during the androgen deprivation treatment and following androgen restoration as indicated. The ^{32}P-labeled PCR products were separated by electrophoresis through a 7% acrylamide gel. Gels were dried *in vacuo* and subjected to autoradiography. The quantitative analysis is described in Materials and Methods. Titrated standards prepared from diluted RNA samples is not shown.

Figure 3. Representative profile of DNA content of LNCaP, CL1, and CL2 cells. LNCaP, CL1, and CL2 cells were grown to 80 % confluence in culture flasks. Cells were stained with propidium iodide, and the nuclei were analyzed for DNA content by flow cytometry. A total of 10,000 nuclei were analyzed from each sample and the percents of cells within G1, S, and G2-M were determined.

Figure 4. Growth profile of LNCaP, CL1, and CL2 cells. Proliferative activity of LNCaP (◆), CL1 (■), or CL2 cells (▲) was determined by A, ^{3}H-thymidine incorporation assay, and B, growth expansion curve (see Materials and Methods).

Figure 5. Colony forming efficiency of LNCaP, CL1, and CL2 cells in cultures. Diluted cells as indicated were seeded in 10 mm Petri dishes. Cells were incubated for 7 days, fixed in 80 % alcohol, stained with 1% crystal violet.

Figure 6. Growth stimulation of human endothelial cells and bone marrow stromal cells by co-culturing with LNCaP or CL cells. Human endothelial cells and bone marrow stromal cells were grown in the presence of LNCaP, CL1 or CL2 tumor lines for 3 days in a co-culture device. The growth of A, endothelial cells and B, bone marrow stromal cells were measured using a ^{3}H-thymidine incorporation assay after removing the co-cultured tumor cells.

Figure 7. Effect of radiation on cell growth. Aliquots of 3 x 10^{4} LNCaP (◆), CL1 (■), or CL2 cells (▲) were seeded in 24-well plates in triplicates. Cells were exposed to various doses of radiation as indicated. Growth effects of radiation on cells was measured by ^{3}H-thymidine incorporation assay and expressed as percentage of growth inhibition compared to untreated control.

Figure 8. Effect of chemothrapeutic agents on cell growth. Aliquots of 3 x 10^{4} LNCaP (◆), CL1 (■), or CL2 cells (▲) were seeded in 24-well plates in triplicate. A, Vinblastin, B, Taxol, or C, Etoposide was added at the indicated concentrations. The chemosensitivity of cells was measured by ^{3}H-thymidine incorporation and expressed as percentage of growth inhibition compared to untreated control.

Figure 9. Tumorigenicity of LNCaP, CL1 or CL2 xenografts in SCID mice. One million cells of LNCaP (●), CL1 (■), or CL2 cells (▲) in 100 μl of RPMI medium were injected subcutaneously into the flanks of A, female and B, male SCID mice (n = 5/proup). Tumor growth was measured at the indicated time table.

Figure 10. Gross pathology of CL1 and CL2 tumors in intact or castrated male mice. A, large tumor masses with bulky lymphadenopathy 5 weeks after intraprostatic injection (5 x 10^4cells/5 μl). Aggressive local invasion have extended to rectum, bladder, seminal vesicles, vertebral column, and distal retroperitoneal lymph nodes is observed. B, large tumor masses 5 weeks after intratibial injection (2 x 10^4 cells/2μl). Aggressive tumor growth with local invasion and metastasis to retroperitoneal lymph nodes (arrow). C, X-ray appearance of massive tumor growth with invasion and destruction of bone tissue by CL tumor. Both CL1 and CL2 tumors but not the parental LNCaP, have the similar pathological characteristics.

Figure 11. Widespread metastatic disease of CL1 visualized by GFP expression under fluorescence microscopy. A, CL1 orthotopic tumor with homogeneous expression of GFP in castrated male mouse. B, metastatic tumor in the retroperitoneal lymph nodes visualized by GFP expression. C, hematogenous/lymphatic skeletal metastases in the femur. Note the intact cortex of the bone. D, GFP expression in lung metastases. E, dense metastatic disease in the liver. F, splenic tumor colonies expressing GFP. G, tumor metastases visualized in the kidney by GFP expression. H, tumor lesions visualized in the brain by GFP expression.

Figure 12. Quantitative RT-PCR analysis of factors associated with tumor progression. RNAs were extracted from LNCaP, CL1, and CL2 cells, and analyzed for quantitative RT-PCR

expression. Titrated standards prepared from diluted RNA sample are not shown. Molecular weights of the PCR products are stated in Materials and Methods.

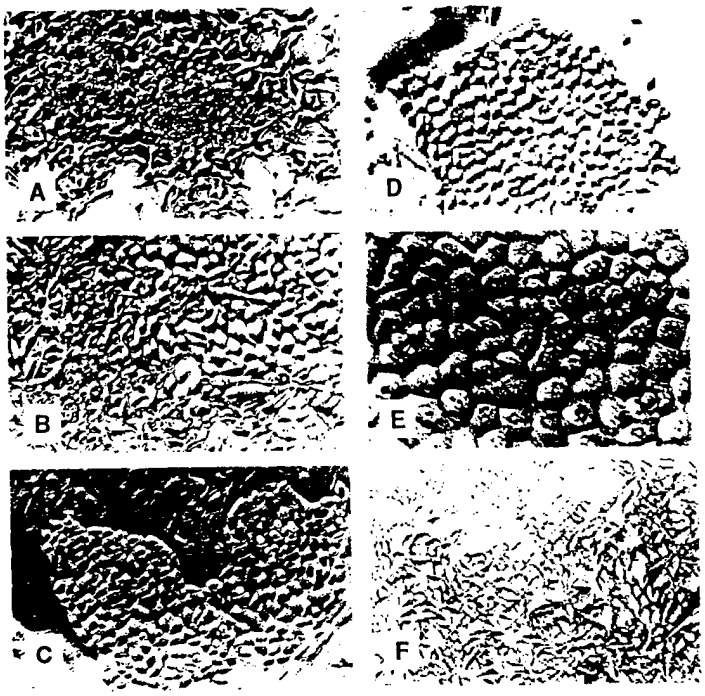

Figure 1

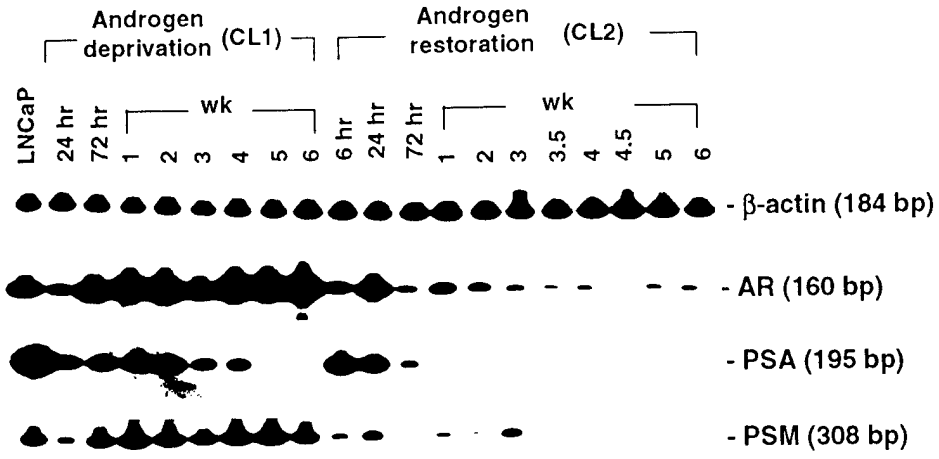
Androgen deprivation (CL1)
Androgen restoration (CL2)
LNCaP
24 hr
72 hr
wk
1
2
3
4
5
6
6 hr
24 hr
72 hr
wk
1
2
3
3.5
4
4.5
5
6
- β-actin (184 bp)
- AR (160 bp)
- PSA (195 bp)
- PSM (308 bp)

Figure 2

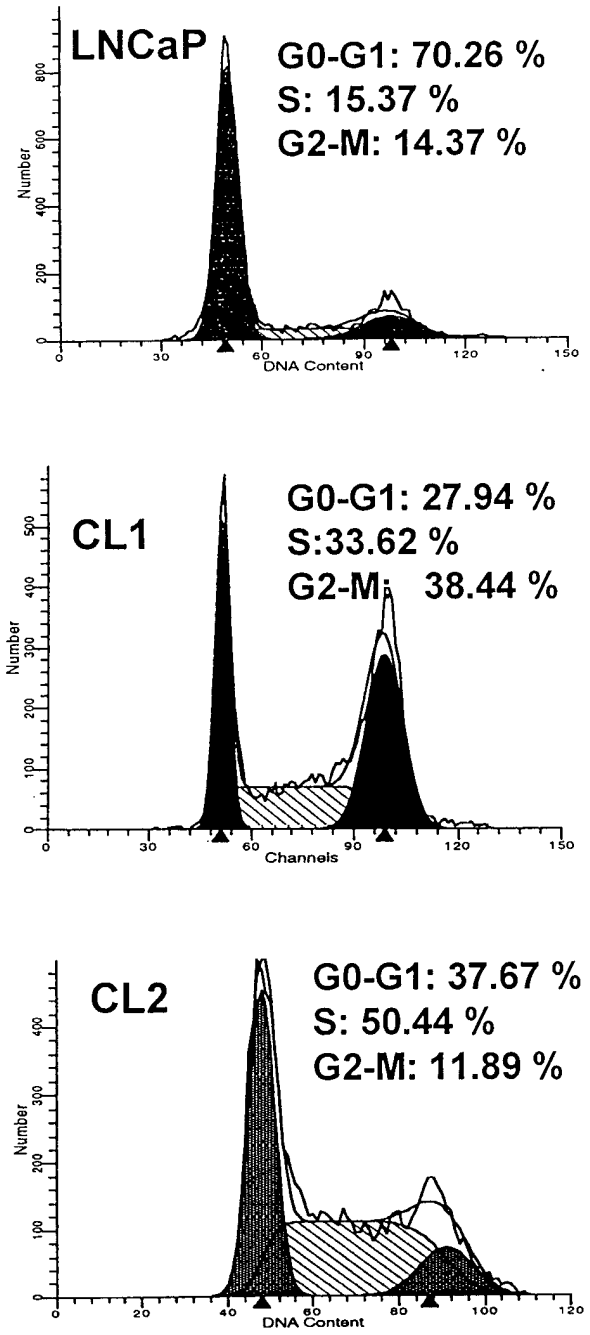
LNCaP
G0-G1: 70.26 %
S: 15.37 %
G2-M: 14.37 %
Number
DNA Content
CL1
G0-G1: 27.94 %
S:33.62 %
G2-M: 38.44 %
Number
Channels
CL2
G0-G1: 37.67 %
S: 50.44 %
G2-M: 11.89 %
Number
DNA Content

Figure 3

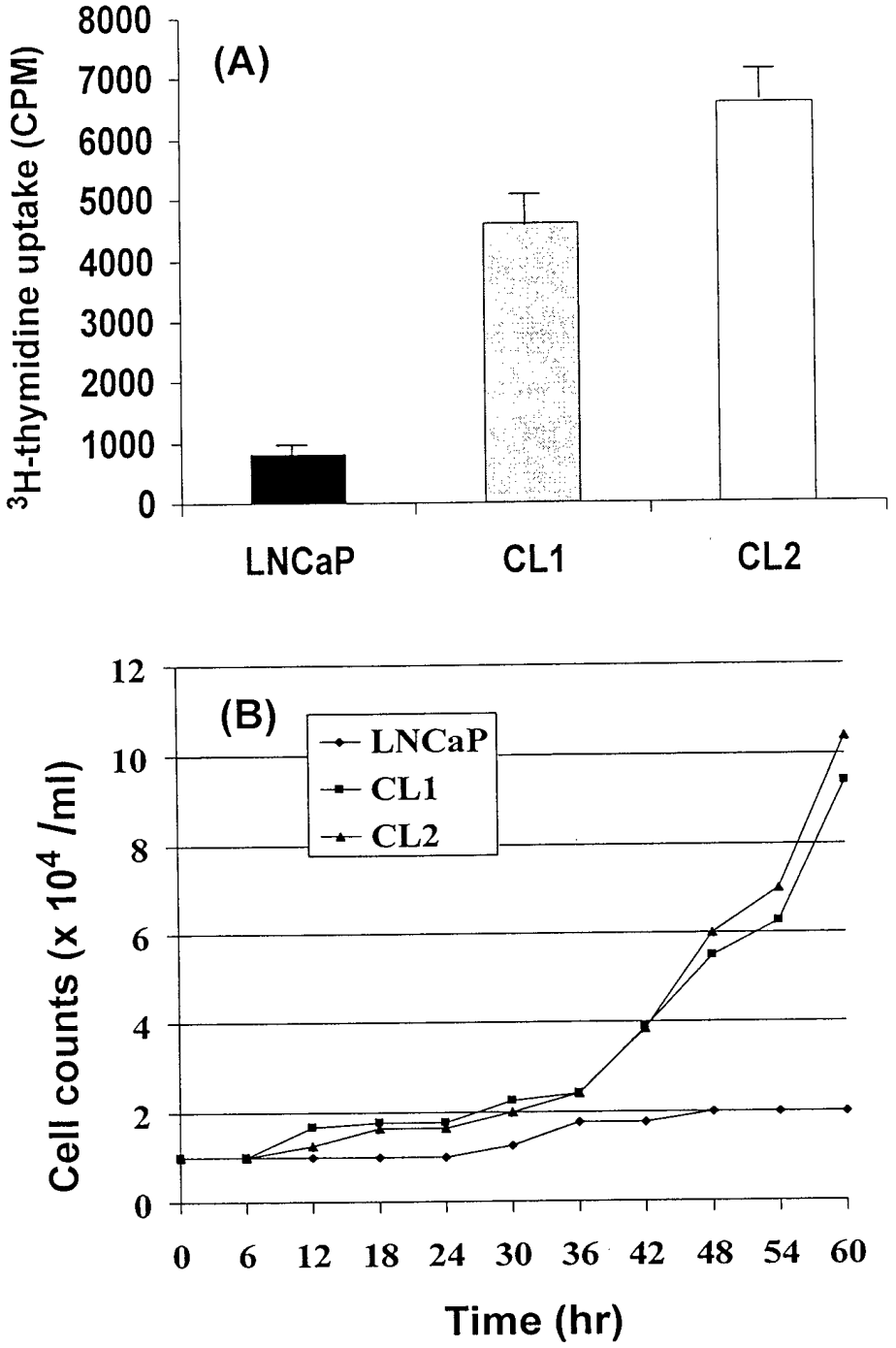
(A)
^{3}H-thymidine uptake (CPM)
8000
7000
6000
5000
4000
3000
2000
1000
0
LNCaP
CL1
CL2
(B)
LNCaP
CL1
CL2
Cell counts (x 10^4 /ml)
12
10
8
6
4
2
0
0
6
12
18
24
30
36
42
48
54
60
Time (hr)

Figure 4

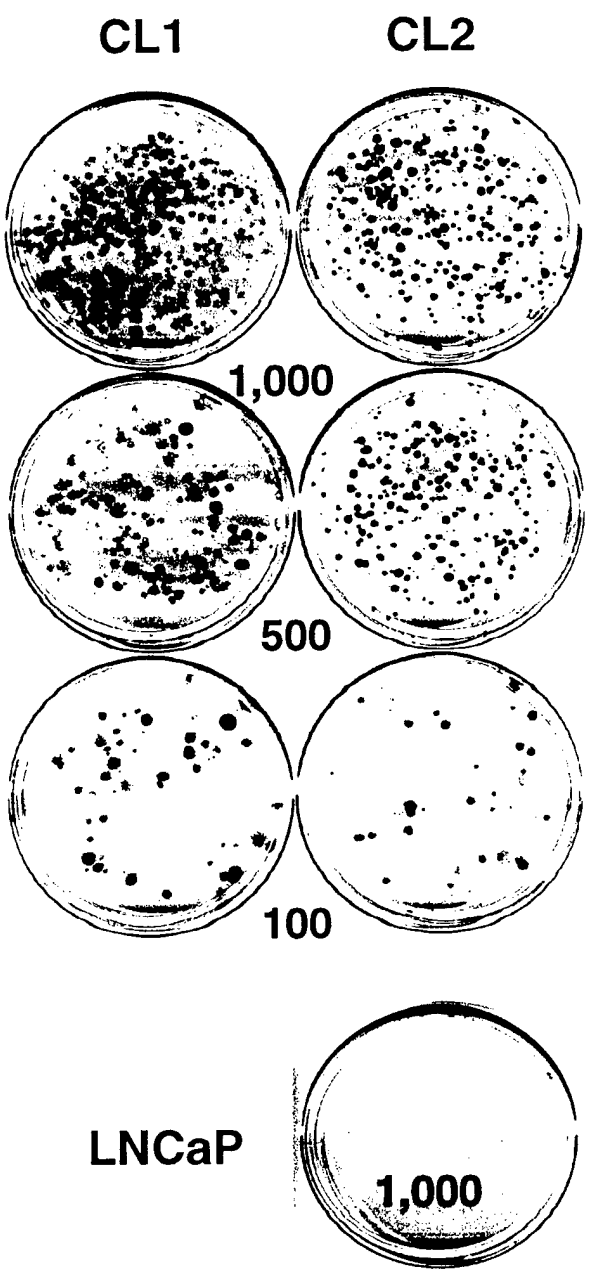

Figure 5

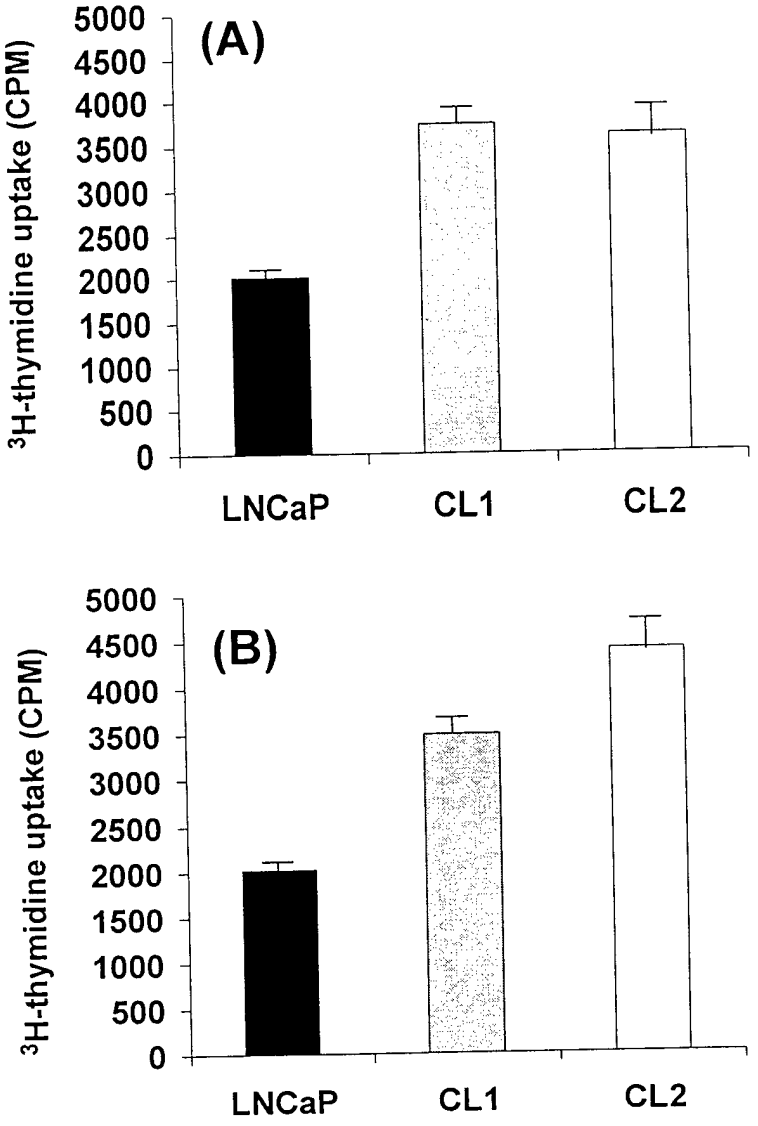
(A)
^{3}H-thymidine uptake (CPM)
5000
4500
4000
3500
3000
2500
2000
1500
1000
500
0
LNCaP
CL1
CL2
(B)
^{3}H-thymidine uptake (CPM)
5000
4500
4000
3500
3000
2500
2000
1500
1000
500
0
LNCaP
CL1
CL2

Figure 6

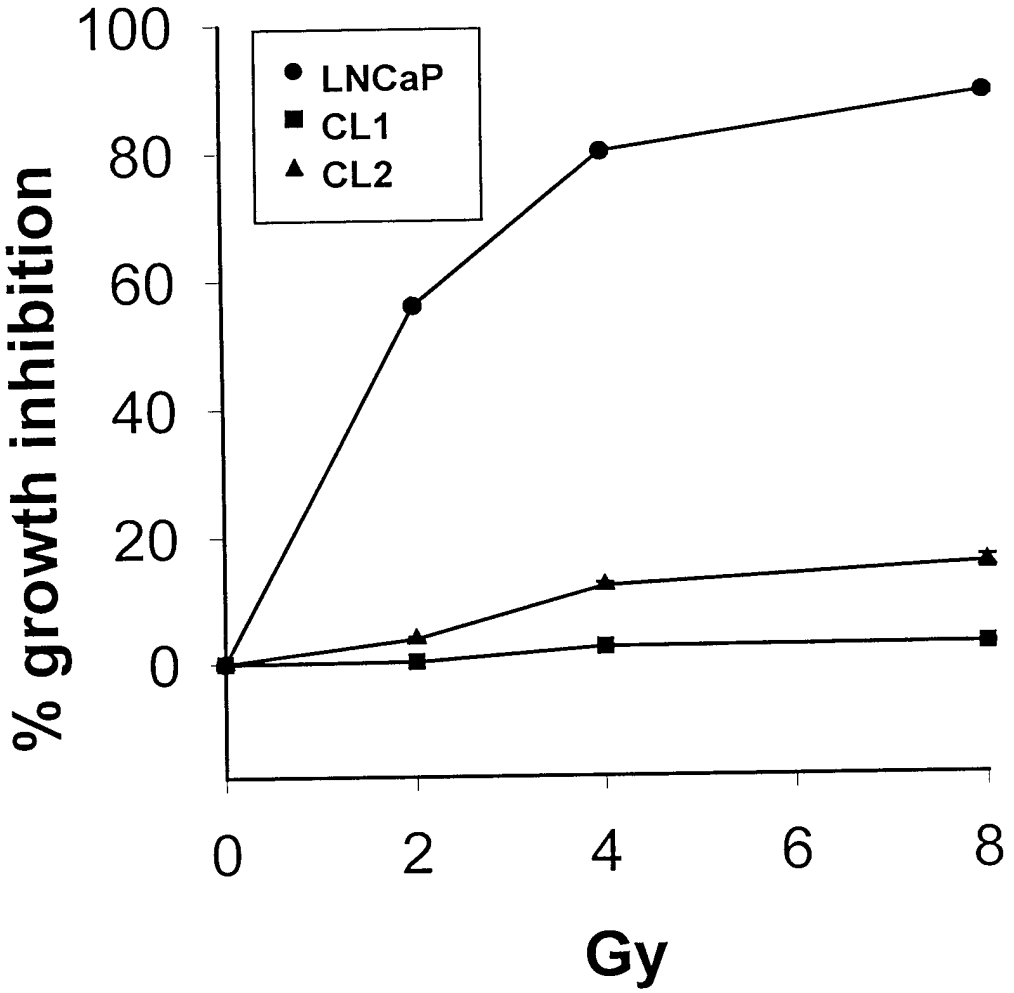

Figure 7

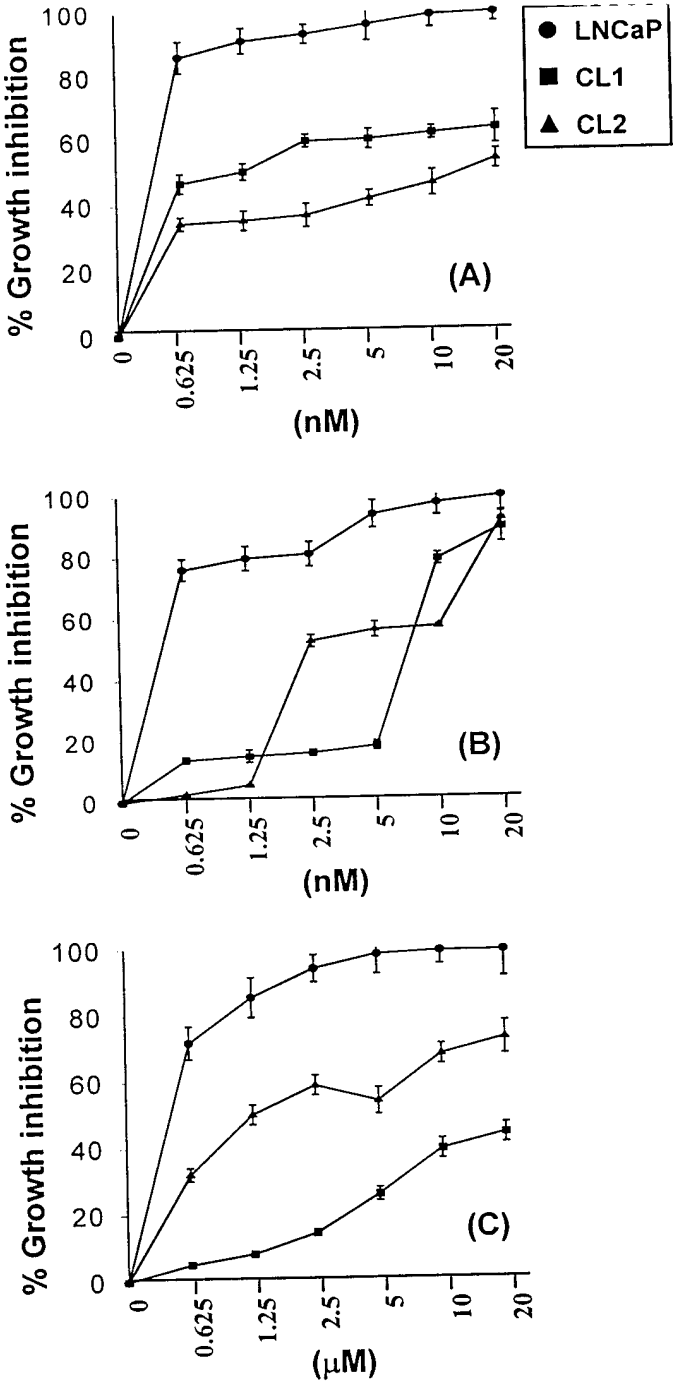
LNCaP
CL1
CL2
% Growth inhibition
100
80
60
40
20
0
(A)
0
0.625
1.25
2.5
5
10
20
(nM)
% Growth inhibition
100
80
60
40
20
0
(B)
0
0.625
1.25
2.5
5
10
20
(nM)
% Growth inhibition
100
80
60
40
20
0
(C)
0
0.625
1.25
2.5
5
10
20
(μM)

Figure 8

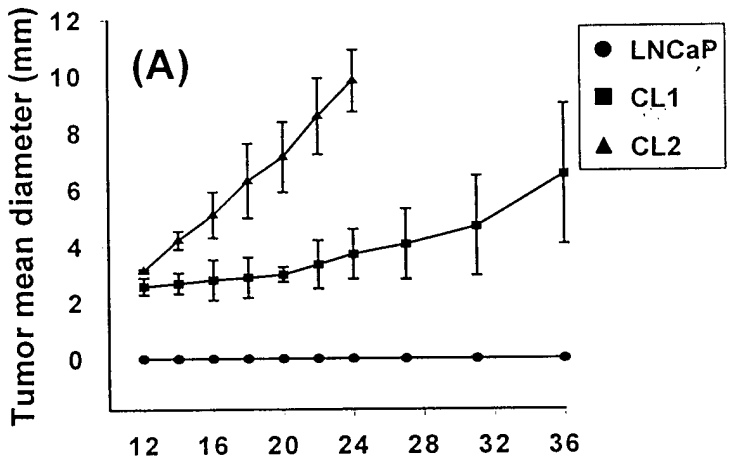
(A)
Tumor mean diameter (mm)
12
10
8
6
4
2
0
12 16 20 24 28 32 36
LNCaP
CL1
CL2

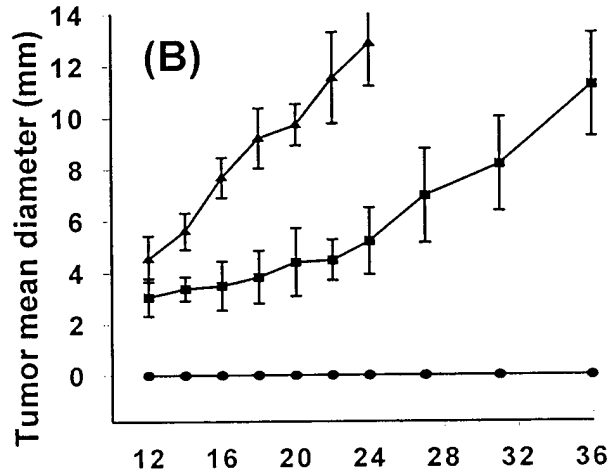
(B)
Tumor mean diameter (mm)
14
12
10
8
6
4
2
0
12 16 20 24 28 32 36

Figure 9

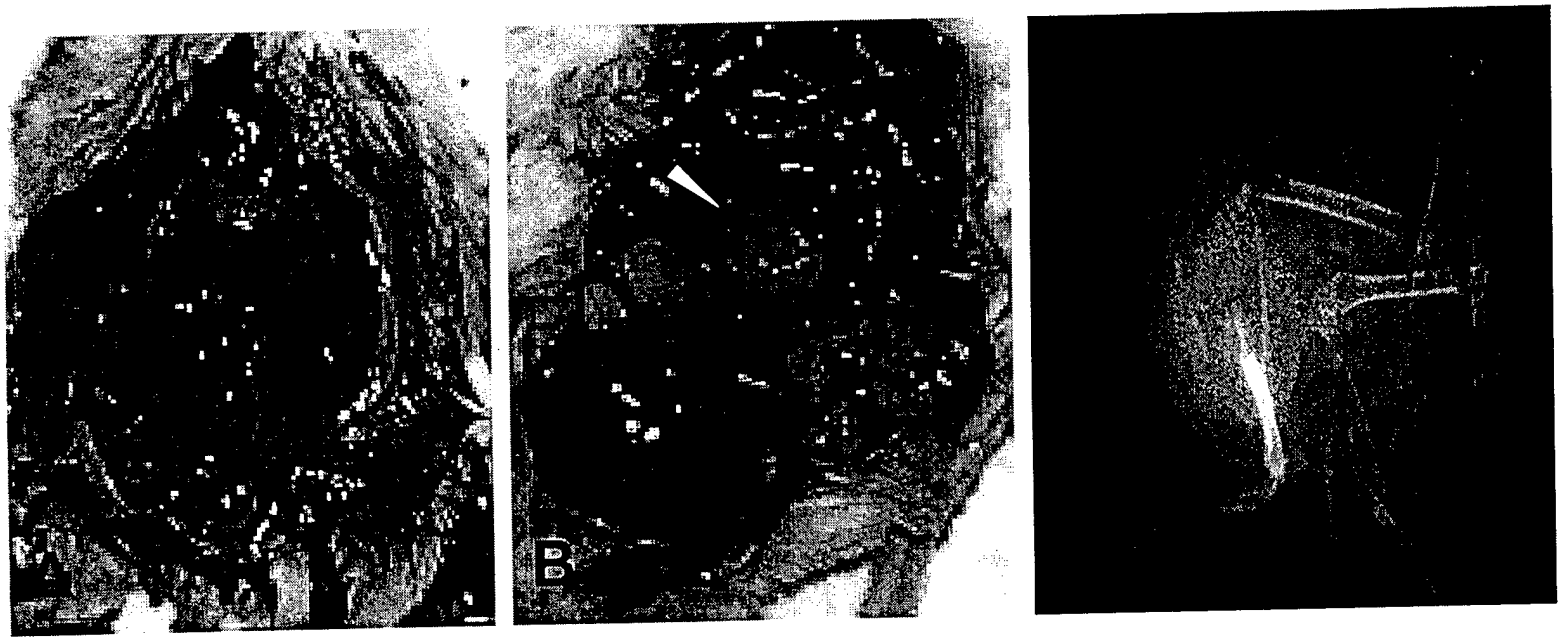

Figure 10

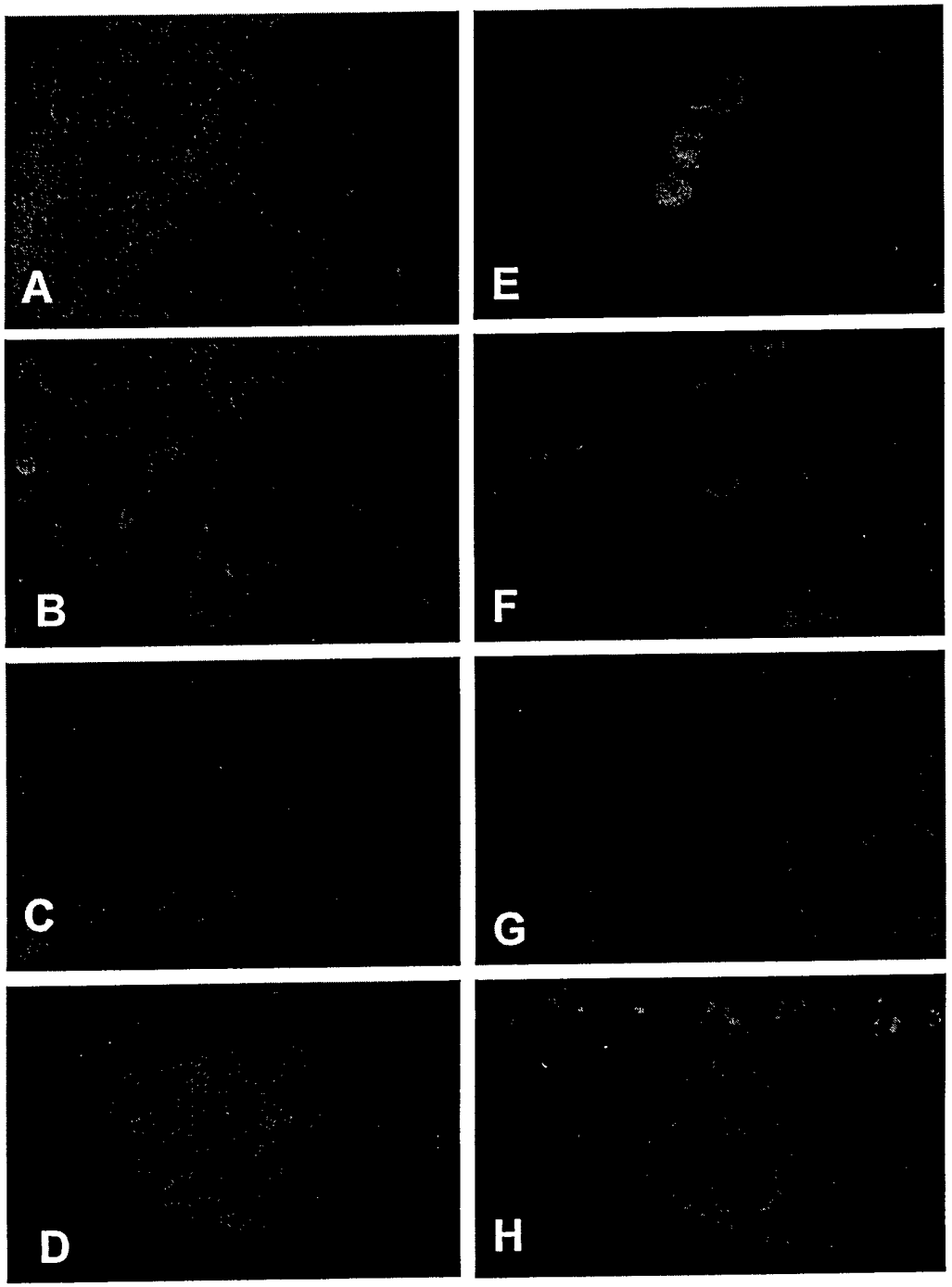

Figure 11

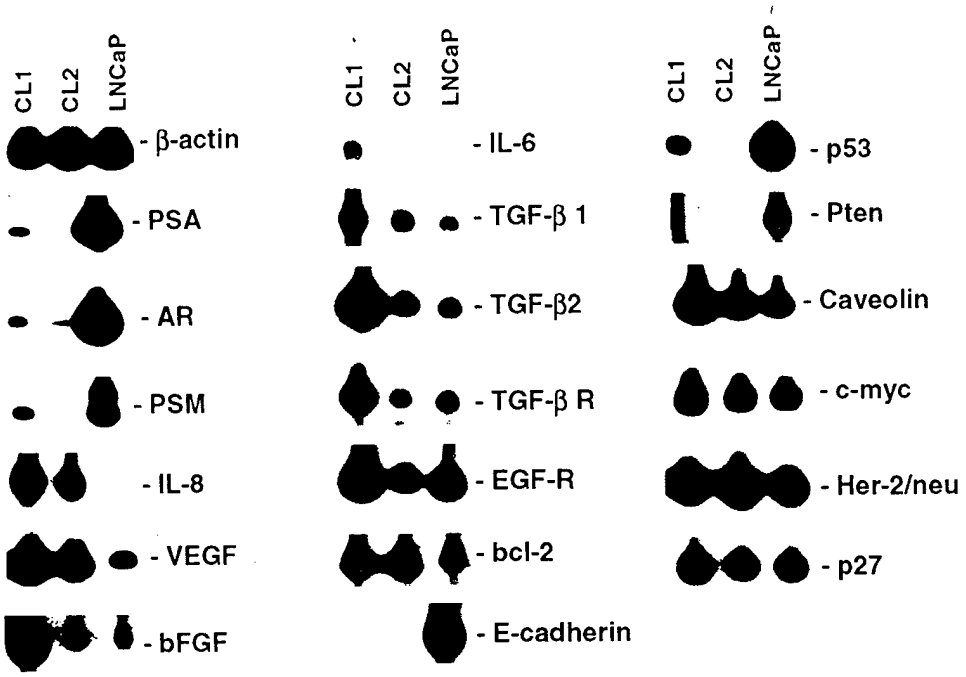
CL1
CL2
LNCaP
- β-actin
- PSA
- AR
- PSM
- IL-8
- VEGF
- bFGF
CL1
CL2
LNCaP
- IL-6
- TGF-β 1
- TGF-β2
- TGF-β R
- EGF-R
- bcl-2
- E-cadherin
CL1
CL2
LNCaP
- p53
- Pten
- Caveolin
- c-myc
- Her-2/neu
- p27

Figure 12